iScience

CellPress
OPEN ACCESS

Article

Cretaceous Blind Snake from Brazil Fills Major Gap in Snake Evolution

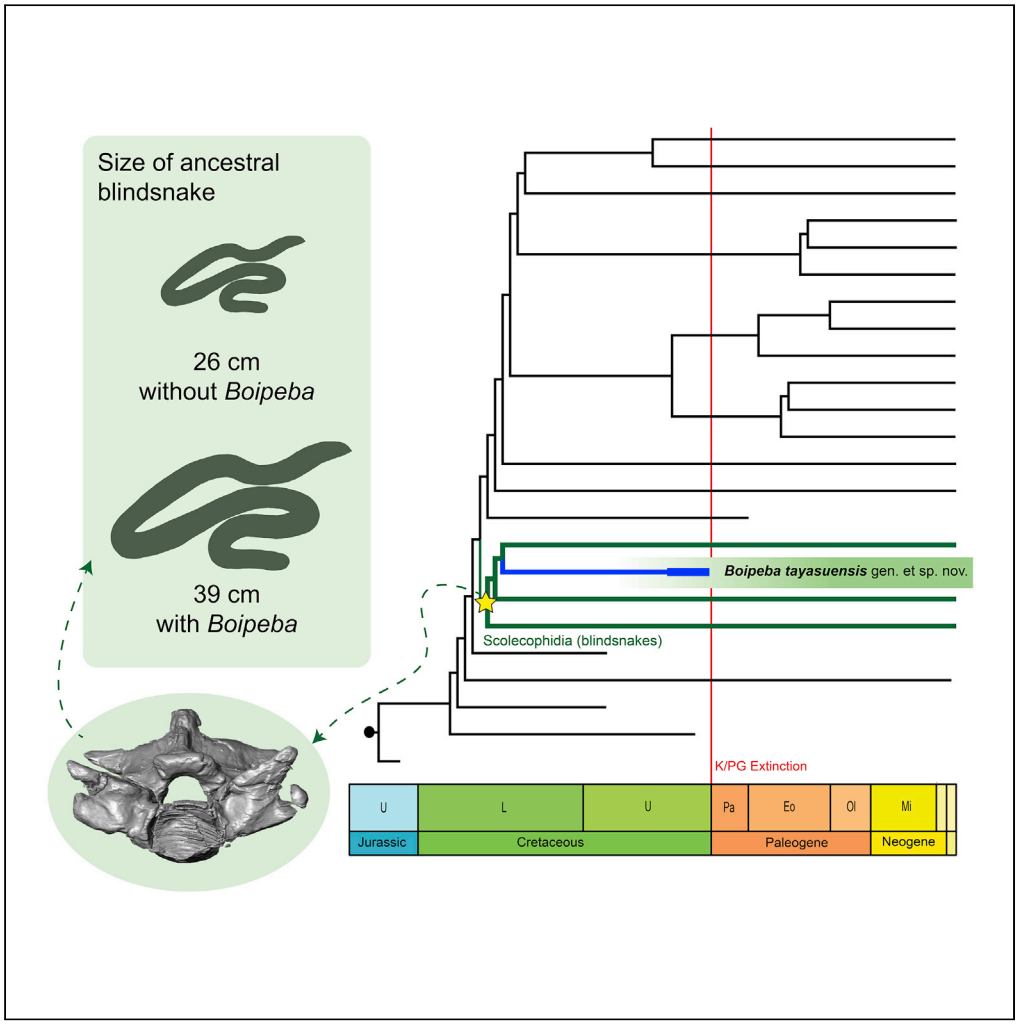

Thiago Schineider Fachini, Silvio Onary, Alessandro Palci, Michael S.Y. Lee, Mario Bronzati, Annie Schmaltz Hsiou

thiagoschineiderf@usp.br (T.S.F.)
silvioonary@usp.br (S.O.)

HIGHLIGHTS

Boipeba tayasuensis is the oldest fossil blind snake from the Late Cretaceous of Brazil

A new phylogenetic analysis places the taxon within living typhlopoids

Boipeba is estimated to be ~1 m in length, larger than any living blind snake

The small body size of extant blind snakes is due to subsequent miniaturization

Fachini et al., iScience *23*, 101834
December 18, 2020
https://doi.org/10.1016/j.isci.2020.101834

iScience

CellPress
OPEN ACCESS

Article

Cretaceous Blind Snake from Brazil Fills Major Gap in Snake Evolution

Thiago Schineider Fachini,[1,5,6,*] Silvio Onary,[1,2,3,5,*] Alessandro Palci,[2,3] Michael S.Y. Lee,[2,3] Mario Bronzati,[4] and Annie Schmaltz Hsiou[1]

SUMMARY

Blind snakes (Scolecophidia) are minute cryptic snakes that diverged at the base of the evolutionary radiation of modern snakes. They have a scant fossil record, which dates back to the Upper Paleocene-Lower Eocene (~56 Ma); this late appearance conflicts with molecular evidence, which suggests a much older origin for the group (during the Mesozoic: 160–125 Ma). Here we report a typhlopoid blind snake from the Late Cretaceous of Brazil, *Boipeba tayasuensis* gen. et sp. nov, which extends the scolecophidian fossil record into the Mesozoic and reduces the fossil gap predicted by molecular data. The new species is estimated to have been over 1 m long, much larger than typical modern scolecophidians (<30 cm). This finding sheds light on the early evolution of blind snakes, supports the hypothesis of a Gondwanan origin for the Typhlopoidea, and indicates that early scolecophidians had large body size, and only later underwent miniaturization.

INTRODUCTION

Snakes comprise one of the most successful radiations of land vertebrates, with over 3,800 living species (Uetz et al., 2020). With ~620 species, blind snakes (Scolecophidia) represent a significant portion of snake diversity (Uetz et al., 2020). They consist of small worm-like snakes, generally less than 30 cm in total length (TL) (Hedges, 2008; Feldman et al., 2016), with adaptations linked to their burrowing lifestyle such as a small subterminal mouth, uniquely modified jaws, reduced eyes covered by a large scale, and a cylindrical body with similar cranial and caudal ends (Cundall and Irish, 2008; Hsiang et al., 2015).

The origin of blind snakes is unclear. Their morphology includes a mixture of seemingly primitive lizard-like features and highly specialized characters (List, 1966), and there is disagreement between morphological and molecular phylogenetic analyses with regard to their phylogenetic position and monophyly (Zheng and Wiens, 2016; Figueroa et al., 2016; Garberoglio et al., 2019a; Caldwell 2019). Furthermore, while most recent molecular analyses agree on the non-monophyly of scolecophidians (but see Singhal et al., 2020), they still disagree on their branching order, with anomalepidids placed either in a more basal or more derived position relative to the other blind snake lineages (Leptotyphlopidae and Typhlopoidea) (Zheng and Wiens, 2016; Figueroa et al., 2016; Miralles et al., 2018). Regardless of this inconsistency, molecular analyses agree that blind snakes are basal to other living snakes, and thus have very ancient origins, sometime between the Upper Jurassic and the Lower Cretaceous (160–125 Ma) (Zheng and Wiens, 2016; Vidal et al., 2010; Burbrink et al., 2020) in Gondwana (Vidal et al., 2010; Pyron and Wallach, 2014). However, the oldest occurrence of scolecophidians in the fossil record currently dates back only to the Upper Paleocene-Lower Eocene (c. 56 Ma) of Europe and northern Africa (Rage, 1984; Augé and Rage, 2006), implying the existence of a large fossil gap. The basal position of blindsnakes with respect to other living snakes also means they provide crucial information on the evolution of living snakes (e.g., da Silva et al., 2018).

Here we report on a giant fossil scolecophidian found in Late Cretaceous sediments from Brazil. This finding sheds new light on the origin of blind snakes, bridging the gap between molecular and paleontological evidence (Zheng and Wiens, 2016; Vidal et al., 2010; Pyron and Wallach, 2014; Burbrink et al., 2020). Furthermore, the new fossil also provides insights into scolecophidian body size evolution, showing that extreme miniaturization is likely a derived trait within these highly specialized snakes, and thus small size cannot be assumed to characterize the ancestral blind snake or the most recent common ancestor of modern (crown) snakes in general.

[1]Laboratório de Paleontologia, Faculdade de Filosofia Ciências e Letras de Ribeirão Preto, Universidade de São Paulo, Ribeirão Preto, São Paulo, Brazil

[2]College of Science and Engineering, Flinders University, Adelaide, SA 5042, Australia

[3]South Australian Museum, North Terrace, Adelaide, SA 5000, Australia

[4]Laboratório de Evolução e Biologia Integrativa, Faculdade de Filosofia Ciências e Letras de Ribeirão Preto, Universidade de São Paulo, Ribeirão Preto, São Paulo, Brazil

[5]These authors contributed equally.

[6]Lead Contact

*Correspondence: thiagoschineiderf@usp.br (T.S.F.), silvioonary@usp.br (S.O.)

https://doi.org/10.1016/j.isci.2020.101834

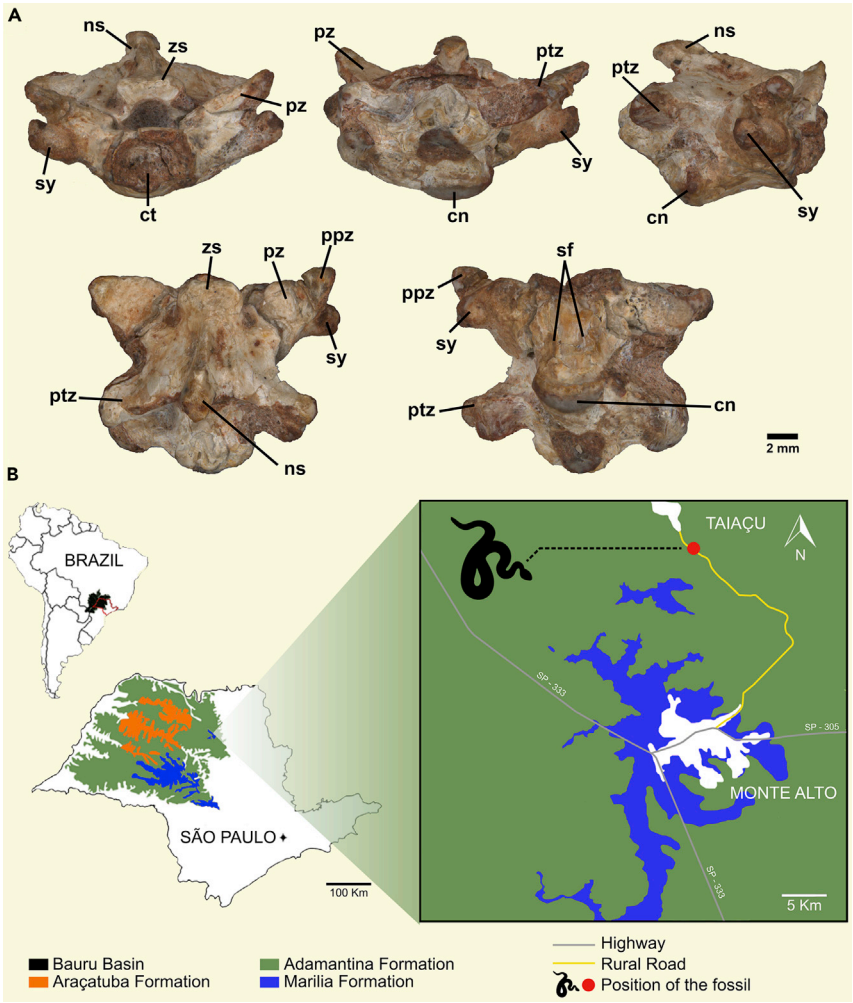

Figure 1. Holotype of *Boipeba tayasuensis*

(A) MPMA 16-0008-08, isolated precloacal vertebra in (upper row) anterior, posterior, and lateral views, respectively, and (lower row) dorsal, and ventral views, respectively.

(B) Geographical and geological map showing the type locality where the fossil material was recovered. Abbreviations: cn., condyle; ct., cotyle; ns., neural spine; ptz., postzygapophysis; ppz., prezygapophyseal accessory processes; pz., prezygapophysis.; sf., subcentral foramina; sy., synapophysis; zs., zygosphene.

RESULTS

Systematic Palaeontology

Squamata Oppel, 1811

Ophidia Brongniart, 1800

Scolecophidia Duméril and Bibron, 1844

Boipeba tayasuensis gen. et sp. nov.

(Figures 1, 2, S1, and S2)

Etymology

Generic epithet comes from the combination of the Brazilian native language Tupi-Guarani, "boi" meaning snake, and "peba" meaning flattened, in reference to the shape of the vertebrae. The species epithet

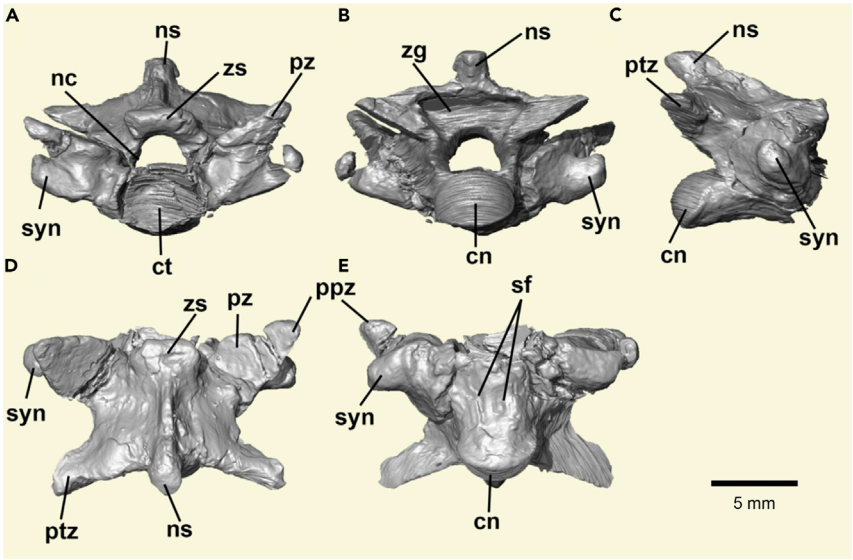

Figure 2. Three-Dimensional Reconstruction of *Boipeba tayasuensis*

(A–E) MPMA 16-0008-08, isolated precloacal vertebra in (A) anterior, (B) posterior, (C) lateral, (D) dorsal, and (E) ventral views. Cn, condyle; ct., cotyle; nc, neural canal; ns., neural spine; ptz., postzygapophysis; ppz., prezygapophyseal accessory processes; pz., prezygapophysis.; sf., subcentral foramina; syn., synapophysis; zg, zygantrum; zs., zygosphene.

"tayasuensis" derives from the type locality where the fossil was found, Taiaçu municipality, São Paulo, Brazil.

Holotype

MPMA 16-0008-08, a single precloacal vertebra with partial successive vertebra (MPMA = Museu de Paleontologia Prof. Antônio Celso de Arruda Campos, Monte Alto, São Paulo State, Brazil).

Locality and Horizon

The fossil comes from a rural road between the municipalities of Monte Alto and Taiaçu, in the Northwest of the state of São Paulo, Brazil (Figure 1B) (S21° O9′53.9″/W48°29′54.0″). The outcrop bearing the new material is a rich fossiliferous locality that preserves an abundant fauna including crocodyliforms (Carvalho et al., 2007; Iori and de Souza Carvalho, 2009; Iori and Carvalho, 2011; Iori and Garcia, 2012; Iori et al., 2013; Iori and Campos, 2017), testudines (Ferreira et al., 2018), and dinosaurs such as sauropods and non-avian theropods (Méndez et al., 2014; Santucci and Arruda-Campos, 2011; Tavares et al., 2014). The sediments in the outcrop consist of the typical reddish muddy sandstones of the Adamantina Formation (Bauru Basin) found in the Monte Alto region (Batezelli, 2017). The time span of the Adamantina Formation has been the matter of a long debate, with some works estimating a Turonian-Santonian age (Dias-Brito et al., 2001), whereas others suggest a younger age, between Campanian-Maastrichtian (Batezelli, 2017; Gobbo-Rodrigues et al., 1999), or a broader range, Cenomanian-Maastrichtian (Menegazzo et al., 2016). There are no integrative absolute date studies for the Adamantina Formation to specify the age correlation among the different fossiliferous localities found in the Bauru Group. Recently, the first high-precision U-Pb geochronology study has shown a post-Turonian maximal age (≤87.8 Ma) for the type stratum of *Brasilestes stardusti* (Castro et al., 2018), which is overlain by the dinosaur-bearing Marília Formation; this age thus constrains the maximum age of the Adamantina Formation at the *Boipeba* site. The minimum age is not well constrained, but presence of non-avian dinosaurs in higher beds implies an age pre-dating the Cretaceous-Paleogene (K/Pg) boundary (66 Ma) (Batezelli, 2017; Menegazzo et al., 2016).

Diagnosis

Medium-sized snake vertebra (~7-mm-anteroposteriorly-long centrum) distinguished from all other ophidians in possessing the following unique combination of vertebral features: dorsoventrally compressed vertebra having oval cotyle and condyle; zygosphene with straight anterior margin; prezygapophyseal articular facets with high angle of inclination (~25°) above the horizontal plane; presence of elongated

prezygapophyseal accessory processes; undivided synapophyses (i.e., no distinct diapophyseal and parapophyseal facets) mediolaterally expanded to the level of the prezygapophyseal articular facets; synapophyses located above the ventral margin of the cotyle; low neural spine slanting posteriorly; shallowly concave posterior margin of neural arch; cylindrical centrum lacking parasagittal ridges and hemal keel (at least in middle/posterior trunk vertebrae, unknown in anterior vertebrae); lack of paracotylar foramina; lack of parazygantral foramina; weak precondylar constriction; and asymmetrical subcentral foramina.

Description

The holotype consists of an isolated vertebra articulated with the anterior region of a fragmentary following vertebra. It is likely to belong to the middle or posterior precloacal region due to the absence of structures such as hypapophyses, lymphapophyses, pleurapophyses, or hemapophyses. The vertebra is three-dimensionally preserved. The neural arch is mediolaterally expanded and dorsoventrally compressed. The zygantrum is deep and has a pair of foramina inside. In dorsal view the neural arch displays a shallowly concave posterior embayment. In ventral view, the centrum is cylindrical, completely smooth (i.e., hemal keel absent), with a weak precondylar constriction. On the ventral surface of the centrum there is a pair of asymmetrical subcentral foramina, where the left foramen is small but distinct, whereas on the right side only a broad shallow fossa is visible, and the foramen has not fully developed through the bone (Figures 2, S1, and S2), a condition found in some other living and fossil scolecophidians (Mead, 2013).

The neural spine is low, posterodorsally inclined, and in dorsal view, extends longitudinally from the posterior region of the zygosphene roof to slightly beyond the posterior embayment of the neural arch. The zygosphene is robust and partly eroded in the three-dimensionally preserved main specimen; however, in the fragmentary successional vertebra it is well preserved and characterized by a rectilinear anterior margin (Figure S1). The neural canal is vaulted.

The prezygapophyseal articular facets are broad, subtriangular in shape, and inclined above the horizontal about 25° (average between left and right sides). Long prezygapophyseal accessory processes are present. The process on the left side is partially worn, but the one on the right is complete (Figures 1 and 2). These processes stand out quite distinctly when two vertebrae (one being a digital replica) are placed in articulation (Figure S2). The synapophyses are undivided (i.e., no distinct para- and diapophyses), extend laterally to the level of the prezygapophyseal articular facets, and are placed dorsal to the ventral margin of the cotyle. Both cotyle and condyle are oval (i.e., dorsoventrally compressed) in anteroposterior view.

Systematic Comparisons to Other Ophidians

Despite the apparent conservative morphology of snake vertebrae, a set of anatomical features can be used to identify them at least to some broad taxonomic level when found in isolation (Rage, 1984). *Boipeba* retains a mix of plesiomorphic features observed in stem snakes together with apomorphic traits typical of some representatives of the crown-group (modern snakes), the clade stemming from the most recent common ancestor of all living snakes (Figures 2 and 3; Table 1). We show below that *Boipeba* is most similar to blind snakes (scoleophidians) and distinct from all other snakes.

Among all the extant and extinct snakes known, *Boipeba tayasuensis* (Figures 2 and 3A) shows a combination of vertebral features that is only observed in modern scolecophidians, most notably in typhlopoids *sensu* Pyron and Wallach (2014) (Figure 3B). The vertebral features that are shared between *Boipeba* and Scolecophidia (Figures 3A and 3B; Table 1) include (1) dorsoventrally flattened vertebra, (2) absence of median notch in the posterior border of the neural arch, (3) narrow and cylindrical centrum, (4) absence of hemal keel and/or median ventral prominence between the cotyle and condyle, (5) presence of asymmetrical subcentral foramina, (6) weakly developed precondylar constriction, (7) cotyle and condyle oval in anteroposterior view, (8) the presence of well-developed prezygapophyseal processes, and (9) undivided synapophyses with no distinction between the para- and diapophyseal articular facets (Rage, 1984). Additionally, modern typhlopoids, exemplified by *Afrotyphlops punctatus* (Figure 3B), exclusively share with *Boipeba* the high position of the synapophyses, which are located dorsal to the ventral margin of the cotyle. Despite the overall similarity, *Boipeba* differs from modern scolecophidians in having a wider and shorter vertebra, synapophyses that extend further laterally, and a taller (though still relatively low) neural spine.

Despite its clear scolecophidian similarities, *Boipeba* also has some features in common with other basal fossil snakes. Early stem snakes, informally termed "parviraptorids" (Caldwell et al., 2015), share with *Boipeba* the

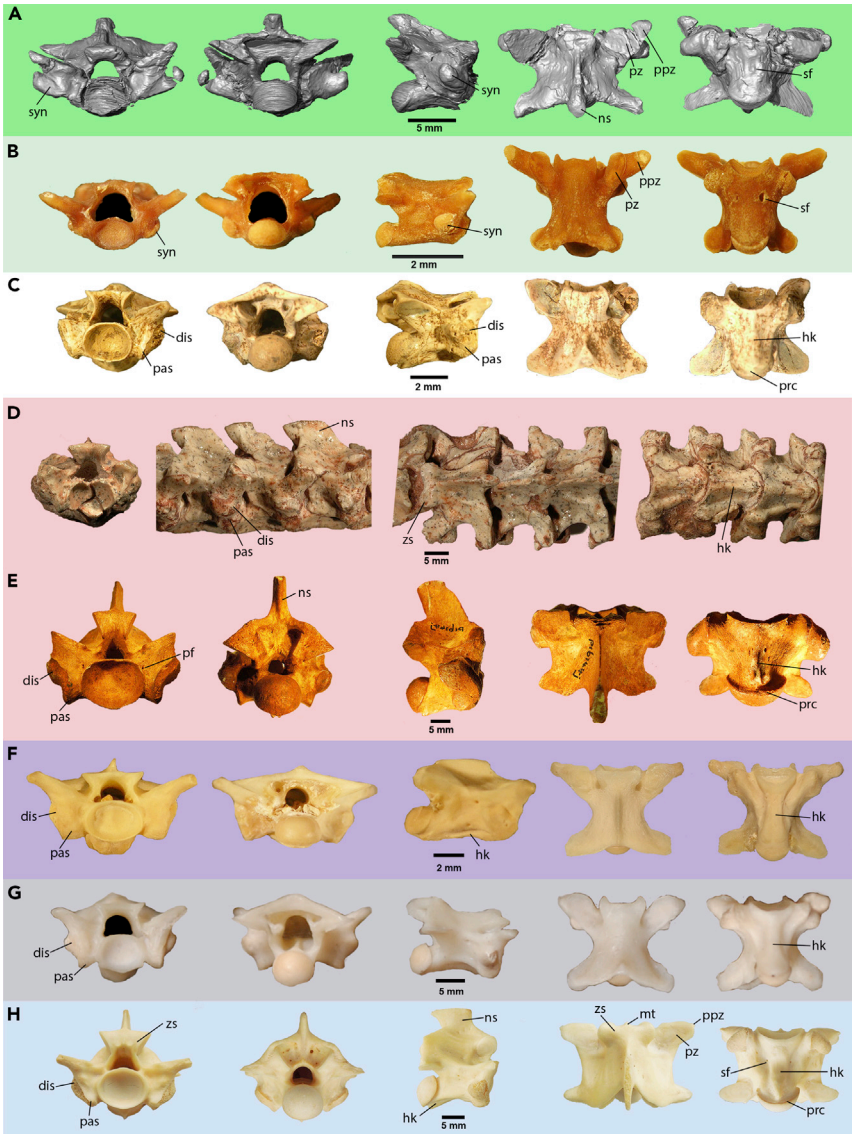

Figure 3. Vertebral Comparisons among *Boipeba tayasuensis* and Selected Ophidian Specimens

Background colors match the groups in Figure 4.

(A) *Boipeba tayasuensis*, 3D model surface rendering (MPMA 16-0008-08).

(B) *Afrotyphlops punctatus* (USNM 320704).

(C) *Coniophis precedens* (UALVP unnumbered specimen).

(D) *Dinilysia patagonica* (MACN-RN unnumbered specimen).

(E) *Wonambi naracoortensis* (SAMA P16168).

(F) *Anilius scytale* (MCZ, 19537).

(G) *Cylindrophis ruffus* (MNHN, 1869 771).

(H) *Simalia amethistina* SAMA R2605.

With the only exception of *Dinilysia*, views from right to left are in anterior, posterior, right lateral, dorsal, and ventral views; anterior, right lateral, dorsal, and ventral for *Dinilysia*. Lateral view was mirrored in *Coniophis* and *Wonambi* for ease of comparison. Abbreviations: dis., diapophyseal articular facet of synapophyses; hk., hemal keel; mt., median tubercle; ns., neural spine; pas. parapophyseal articular facet of synapophyses; pcr., precondylar constriction; pf., paracotylar foramen; ppz., prezygapophyseal processes; pz., prezygapophysis; sf., subcentral foramen; syn., synapophysis; zs., zygosphene.

Vertebral Traits	*Boipeba tayassuensis*	Scolecophidia (*Afrotyphlops punctatus*)	*Coniophis precedens*	*Dinilysia*	Madtsoiidae (*Wonambi naracoortensis*)	*Anilius scytale*	Macrostomata (*Simalia amethistina*)
Confluent synapophyses	Present*	Present*	Absent	Absent	Absent	Absent	Absent
Synapophyses in the same level of prezygapophyseal articular facets	Present	Absent	Absent	Absent	Present	Absent	Absent
Presence of long prezygapophyseal accessory processes	Present	Present	Absent	Absent	Absent	Present	Absent
Dorsoventrally flattened neural arch	Present	Present	Present	Absent	Absent	Present	Absent
Shallow posterodorsal margin of the neural arch	Present	Present	Present	Present	Absent	Present	Absent
Low neural spine	Present	Present	Present	Absent	Absent	Present	Absent
Cylindrical: centrum	Present	Present	Present	Absent	Absent	Absent	Absent
Smooth ventral margin of the centrum	Present*	Present*	Absent	Absent	Absent	Absent	Absent
Ellipsoidal dorsoventrally compressed cotyle	Present	Present	Variable	Variable	Absent	Absent	Absent
Asymmetrical subcentral foramina	Present	Present	Absent	Present	Absent	Present	Absent

Table 1. Comparative Vertebral Traits between Selected Ophidian Taxa

*Morphological traits exclusively shared between *Boipeba tayasuensis* and scolecophidians.

presence of a smooth ventral margin on a cylindrical centrum and the weakly developed precondylar constriction. However, unlike *Boipeba*, "parviraptorids" display very small zygantra and zygosphenes, rounded cotyles and condyles, tall neural spines, absence of prezygapophyseal accessory processes, very steep pre- and postzygapophyseal facets (~40 above horizontal), and synapophyses subdivided into para- and diapophyseal facets (Caldwell et al., 2015). Madtsoiid snakes (e.g., *Wonambi*, Figure 3E), as well as the South American Late Cretaceous stem-snakes *Dinilysia* (Figure 3D, Table 1) and the hind-limbed *Najash* share with *Boipeba* features like the synapophyses extending approximately to the same level of the lateral margin of the prezygapophyseal articular facets, and a shallowly concave posterior margin of the neural arch embayment. However, these stem-snakes differ from *Boipeba* in possessing a well-developed neural spine, rounded cotyle and condyle, prominent hemal keel in a subtriangular centrum with a marked constriction, presence of paired parazygantral foramina (only in madtsoiids and *Najash*), synapophyses with division between the para- and diapophyseal facets, absence of prezygapophyseal accessory processes, and the occurrence of parasagittal and arqual ridges in the neural arch (Zaher et al., 2009; Laduke et al., 2010; Garberoglio et al., 2019a).

The fossil snake *Xiaophis myanmarensis* (Xing et al., 2018), albeit most likely a neonate, presents mid-trunk vertebrae that are remarkably similar to those of *Dinilysia* in general proportions. *Xiaophis* shares with *Boipeba* the presence of low and posteriorly tilted neural spines but can be readily distinguished by the

presence (in *Xiaophis*) of synapophyses that are subdivided into para- and diapophyseal facets, distinct hemal keels, and smaller prezygapophyseal processes. The last feature may be due to the early ontogenetic stage of the snake, whereas the other two features cannot be so readily explained.

The only unambiguous Cretaceous ophidian record from the Cenomanian of Brazil, the stem-snake *Seismophis septentrionalis* (Hsiou et al., 2014) shares with *Boipeba* the vaulted neural canal morphology, the relatively low neural arch (in posterior view), and the weakly developed neural spine, but is clearly distinguished from the latter in possessing a flattened hemal keel, presence of parazygantral foramina, rounded cotyle and condyle, and marked parasagittal ridges.

The long-bodied squamate *Tetrapodophis* from the Early Cretaceous of Brazil, which was described as a stem-snake (Martill et al., 2015; but see Caldwell et al., 2016, Paparella et al., 2018, and Caldwell, 2009 for an alternative interpretation), shares with *Boipeba* features such as the low neural spine and neural arch, but differs from the latter in possessing a deep V-shaped posterior margin of the neural arch, divided synapophyses, and the presence of well-defined hemal keels and subcentral fossae. In contrast, *Boipeba* possesses a shallow posterodorsal embayment of the neural arch, undivided synapophyses, and a smooth ventral surface of the centrum.

The Cretaceous (Cenomanian) marine Tethyan Pachyophiidae are characterized by pachyostotic vertebrae, a diagnostic feature not observed in *Boipeba*. Moreover, pachyophiids lack prezygapophyseal processes, which are well developed in *Boipeba*.

Another aquatic fossil snake from the Upper Cretaceous (Cenomanian) of Venezuela, *Lunaophis aquaticus* (Albino et al., 2016), shares with pachyophiids the presence of pachyostosis and the lack of prezygapophyseal processes and has a distinct hemal keel and an elongate subtriangular centrum in ventral view. Thus, *Lunaophis* can also be readily distinguished from *Boipeba*.

The Cretaceous fossil snake *Coniophis precedens* (Figure 3H) shares with modern scolecophidians (Figure 3C) and *Boipeba* (Figures 2 and 3A), features such as the dorsoventrally compressed vertebra, oval cotyle and condyle, relatively low neural spine, narrow centrum, and weak precondylar constriction. However, the absence of prezygapophyseal processes and a flattened hemal keel surrounded by subcentral groves make this extinct snake morphologically different from both scolecophidians and *Boipeba*.

Among alethinophidians, i.e., modern (crown) snakes apart from blind snakes, *Boipeba* shares some features with members of the "Amerophidia" (i.e., *Anilius* + *Tropidophis*) and Uropeltoidea (Figures 2F and 2G), like the dorsoventrally compressed vertebral morphology, a shallowly concave posterior neural arch margin (in dorsal view), the relative steep inclination of the prezygapophyseal articular facets, the presence of well-developed prezygapophyseal accessory processes, zygosphene morphology characterized by a straight anterior edge, and a low neural spine (only in *Anilius*). On the other hand, both amerophidians and uropeltoids are distinct from *Boipeba* in displaying division between the articular facets of the synapophyses, distinctly trifoliate neural canal morphology, flattened hemal keel delimited by subcentral grooves, rounded cotyle and condyle, and subtriangular centrum with marked precondylar constriction. Furthermore, *Boipeba* differs from *Cylindrophis* (Figure 2F) due to the presence of a neural spine (absent in the latter) and from *Anilius* (Figure 2G) in having the neural spine that extends posteriorly beyond the posterior margin of the neural arch.

The vertebrae of afrophidian snakes (i.e., Henophidia + Caenophidia) differ from those of *Boipeba* in many respects. In general, Henophidia (e.g., boids and pythonids like *Simalia amethistina*; Figure 2H) sharply differ from the Cretaceous fossil due to a well-developed neural spine, broad and vaulted neural arch (in posterior view) with marked parasagittal ridges and a deep posterodorsal notch, massive zygosphene with median tubercle (in some species), synapophyses subdivided in para- and diapophyses, rounded cotyle and condyle, prezygapophyseal accessory processes reduced to a small pyramidal projection, variable presence of paracotylar and neural arch foramina (sensu Onary and Hsiou, 2018), weak interzygapophyseal constriction, pre- and postzygapophyseal facets that are typically inclined between 0° and 15° above horizontal (steeply inclined in *Boipeba*, ~25°), and a broad subtriangular centrum with prominent hemal keel and strong precondylar constriction. *Boipeba* shares with members of the Caenophidia (e.g., Colubroidea) the presence of elongated prezygapophyseal processes. However, colubroids have lightly built, elongated vertebrae, synapophyses subdivided into para- and diapophyses, frequent presence of paracotylar foramina, low inclination of the pre- and postzygapophyseal facets, and retain hypapophyses throughout the vertebral column (Rage, 1984).

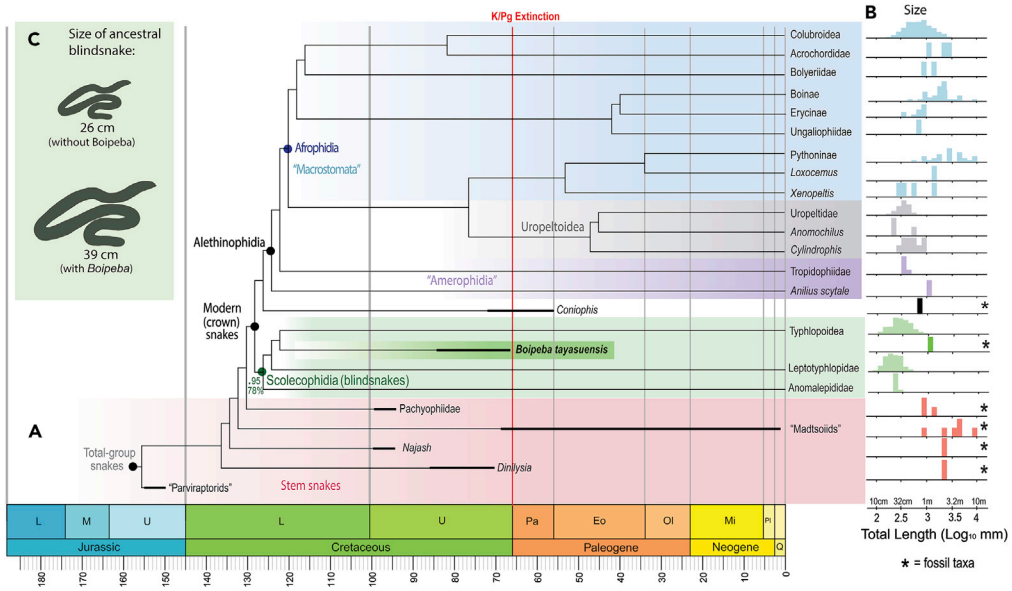

Figure 4. *Boipeba* and the Evolution of Snakes

Taxon shading colors match the scheme in Figure 3.

(A) Phylogenetic relationships of the giant fossil blind snake *Boipeba* and other major snake lineages, based on Bayesian and parsimony analyses of morphology and DNA (tree topology as in Figure S3A; numbers at blind snake clade are Bayesian posterior and parsimony bootstrap support. Divergence dates for living snakes are based on molecular dates (for compatible clades) in Zheng and Wiens (2016); bold lines indicate stratigraphic range or uncertainty for fossil taxa. Quotes denote non-monophyletic taxon names.

(B) Size distribution of all species for each major living snakes lineage and important fossil taxa, on a log scale; note *Boipeba* is larger than living blind snakes.

(C) *Boipeba* greatly increases the size estimate for the most recent common ancestor of living blind snakes (see also Figure S9).

Phylogeny

All vertebral features present in *Boipeba* are fully consistent with what is found in Serpentes, and in particular modern and fossil scolecophidians (List, 1966; Rage, 1984; Mead, 2013); no other vertebrate group is remotely similar. We thus tested the phylogenetic relationships of *Boipeba* by inserting it into a morphological data matrix for the major lineages of living and fossil snakes, expanded from a recent study (Garberoglio et al., 2019b see Methods). *Boipeba* could be scored for 29 vertebral characters out of the 253 morphological characters (see Transparent Methods section). This morphological matrix was analyzed alone, and in combination with DNA data (for living taxa) consisting of 18,753 base pairs from 17 genes (7 mitochondrial and 10 nuclear) from Tonini et al. (2016). Analyses used maximum parsimony (PAUP, Swofford and Sullivan, 2003, and TNT, Goloboff et al., 2008) and undated Bayesian (MrBayes, Ronquist et al., 2012) optimality criteria (see Transparent Methods). Initial analyses with all 37 terminal taxa had support deflated due to "wildcard" taxa with large amounts of missing data, so additional analyses included only the 33 most complete taxa (excluding 4 taxa with >90% missing data). Regardless of the optimality criteria employed or the character/taxon sampling (morphology alone or combined molecular and morphological data, all taxa or fragmentary/contentious taxa excluded), *Boipeba tayasuensis* always emerged unambiguously with scolecophidian affinities, and thus within crown snakes (see Figures 4A and S3–S5). For instance, in the combined morphological and molecular analyses of all 37 taxa (excluding *Tetrapodophis*), support uniting *Boipeba* with all scolecophidians was 72% (parsimony partitioned bootstrap) and 0.99 (Bayesian posterior probability). Within scolecophidians, *Boipeba* was the sister taxon to typhlopoids (here represented by *Typhlops*), but this relationship was not robust (51% bootstrap, 0.65 posterior probability).

There are three unambiguous morphological synapomorphies uniting *Boipeba* with Scolecophidia: the presence of a confluent synapophysis (character 116), the presence of elongated prezygapophyseal accessory processes (character 117), and a smooth ventral margin of the centrum (character 121). Furthermore,

Figure 5. Life Reconstruction of *Boipeba tayasuensis*

This large Cretaceous blind snake inhabited the arid palaeoenviroment of the Bauru Basin, Brazil, alongside titanosaur sauropods, theropods, and terrestrial crocodiles such as *Montealtosuchus* (Mesoeucrocodylia, Peirosauridae). The latter was found in the same outcrop as *Boipeba*. Reconstruction by Jorge Blanco.

the position of the synapophyses placed dorsal to the ventral margin of the cotyle (character 249) is a synapomorphy shared between *Boipeba* and Typhlopoidea. Thus, despite being represented only by vertebral characters, the analyses support a scolecophidian affinity of *Boipeba*.

With regard to the relationships among other snakes, our preferred topology (Figure 4A) is similar to that presented in Garberoglio et al. (2019b), where "parviraptorids" are the earliest diverging stem snakes, followed by *Dinilysia*, *Najash*, the paraphyletic assemblage "madtsoiids," and the marine Pachyophiidae; the last taxon is the sister group to crown-snakes. The North American Cretaceous fossil *Coniophis precedens* was weakly recovered as the sister taxon to the Alethinophidia, *contra* Longrich et al., (2012a), who found it to be the sister taxon to all extant snakes (crown-snakes). *Tetrapodophis* (Martill et al., 2015) was initially excluded from our phylogenetic analyses of snakes due to ongoing debate over its status as a snake (Caldwell et al., 2016; Paparella et al., 2018; Caldwell, 2019). However, we also repeated all analyses adding *Tetrapodophis* to the snake ingroup, as a candidate early snake (Martill et al., 2015). The resulting topologies still retrieved *Boipeba* in the same position within Scolecophidia, and with slightly increased parsimony support (76% partitioned bootstrap) and similar Bayesian support (0.99 PP) (Figures S6–S8).

Size estimate of Boipeba and the Ancestral Scolecophidian

The fossil snake *Boipeba tayasuensis* has a centrum length (CL) of 6.8 mm (measured along the ventral margin), which is very large compared with the minute vertebrae typically found in extant scolecophidians (List, 1966) (see also Data S1). We estimated the total length of *Boipeba* by using the relationship between total length and vertebral length found in extant scolecophidians (see Methods). We obtained an average estimate of total length of 1.1 m for *Boipeba* (Figure 4B and Data S1). When compared with other fossil snakes, *Boipeba* is similar in length to pachyophiids and *Najash* (~1 m), about half the length of *Dinilysia* (~2 m), and is considerably shorter than most "madtsoiids," which have an average total length of about 4.4 m (Figure 4B). The fossil snake *Coniophis* has an estimated TL of about 0.7 m (Longrich et al., 2012a), which is shorter than the estimated TL of *Boipeba* (1.1 m).

Among basal alethinophidians, *Boipeba* is similar in length to *Anilius*, whereas double the length of most tropidophiids and uropeltids (Figure 4B). Afrophidian snakes (i.e., Henophidia + Caenophidia) exhibit a

wide range of sizes within each clade. Colubroid caenophidians have an average size that is smaller (~0.8 m) than that of *Boipeba* (Figure 4B), whereas some henophidian groups such as Boinae and Pythoninae, which include the largest extant snakes, are on average about two to three times longer (average TL of Pythoninae ~2 m; average TL of Boinae ~3 m; Figure 4B) (Feldman et al., 2016).

Boipeba therefore represents an exceptionally large extinct scolecophidian, four times longer than the average anomalepidid (~0.25 m), about five times the average leptotyphlopid (~0.20 m), and nearly three and a half times the average typhlopoid (~0.31 m). It is much closer in size to typical alethinophidians, as well as to most basal fossil snakes (Figure 4B).

The size and phylogenetic position of *Boipeba* sheds substantial light on the evolution of body size within scolecophidian snakes. We reconstructed the size (TL) of the ancestral blind snake using a dated, well-sampled (98 extant species) phylogeny of Scolecophidia (Zheng and Wiens, 2016) and size (TL) data from Feldman et al. (2016). *Boipeba* was inserted into this phylogeny midway along the relevant branch (sister taxon to typhlopoids), and size estimates for all ancestral nodes were obtained using parsimony/likelihood methods (see Methods). When *Boipeba* is included, the ancestral scolecophidian is estimated to have had a total length of about 0.39 m (see Methods, Figures 4C and S9), whereas the analysis using only living scolecophidian taxa retrieved an estimated ancestral body length of only 0.26 m (see Transparent Methods section). This 1.5-fold length increase would translate to a ~3-fold mass increase assuming isometry ($1.5^3 = 3.375$). The TL estimate for the ancestor of living typhlopoids is similarly affected, with an estimate of 0.40 m when the fossil is included in the analysis versus an estimate of 0.30 m when it is excluded (see Transparent Methods section).

DISCUSSION

Boipeba tayasuensis sheds light on important aspects of the early evolution of blind snakes in terms of timing, geographic origin, and body size. Before the discovery of *Boipeba*, the oldest scolecophidians were known from the Eocene of Europe (Rage, 1984) and the Paleocene of Morocco (Augé and Rage, 2006). Thus, *Boipeba* provides the first evidence for their presence in the Mesozoic (Figure 5), extending the fossil record of the group back in time by at least ~10 Ma, and possibly more (up to ~28 Ma, depending on the uncertainty surrounding the age of the Adamantina Formation). The results of the phylogenetic analysis presented here (Figure 4), which recovers *Boipeba* as the sister group to the Typhlopoidea, is consistent with molecular estimates for the origin of the group during the Cretaceous (Zheng and Wiens, 2016; Pyron and Wallach, 2014; Burbrink et al., 2020).

The presence of *Boipeba* in South America has implications for the biogeographic history of the Typhlopoidea, supporting a possible western Gondwana (South American) origin for the group (e.g., Pyron and Wallach, 2014), instead of an eastern Gondwana (India-Madagascar) origin followed by the breakup of Pangaea (contra ref. Vidal et al., 2010). This fossil finding together with the recent studies on molecular divergence age estimates (Pyron and Wallach, 2014; Zheng and Wiens, 2016) is most consistent with a Cretaceous (~122 Ma) rather than the initially hypothesized Middle Jurassic age for the clade (~150 Ma) proposed by Vidal et al. (2010).

The position of Boipeba on the typhlopoid lineage means that it can be used as a calibration (66–87.8Ma) for the minimum age of the typhlopoid-leptotyphlopid divergence, in molecular divergence studies.

Boipeba tayasuensis is estimated to have been slightly over 1 m in TL, a giant among scolecophidians, which are typically less than 30 cm (Hedges, 2008; Feldman et al., 2016) (Figures 4B and 4C). Its size is more comparable to that of typical alethinophidians (excluding boas and pythons), as well as of some early fossil stem snakes (Figure 4 and Data S2). This unusually large size provides insights into the early evolution of body size in blind snakes, suggesting that the ancestral scolecophidian was a sizable snake. When *Boipeba* is included in analyses, the estimated total length of 39 cm of the scolecophidian ancestor is considerably larger than the average TL of extant members of the clade; the same applies to the estimated total length of the ancestral typhlopoid (40 cm). This scenario is even more dramatic when considering the most recent common ancestor (MRCA) of *Boipeba* and Typhlopoidea, where the ancestral state reconstruction produced a TL estimate of 51 cm, nearly twice the length of the average living typhlopoid (see Results and Figure S9). Thus, the miniaturized body plan of modern scolecophidians represents a trait that evolved later in the group, rather than its ancestral condition. Furthermore, our ancestral state reconstruction suggests that miniaturization evolved independently in the three blind snake

lineages (Anomalepididae, Leptotyphlopidae, and Typhlopoidea: Figure S9), as previously suggested by some molecular studies (e.g., Harrington and Reeder, 2017).

Living blind snakes that approach the size of *Boipeba* are extremely rare and include members of the typhlopoids such as the two closely related African species *Afrotyphlops schlegelii* and *Afrotyphlops mucruso*, which can achieve a TL of almost 1 m (List, 1966; Broadley and Wallach, 2009). However, in the Cretaceous such large size may have been more common, if not the norm, for early scolecophidians; the small size of post-Cretaceous forms might be due to the strong selective pressure imposed by the K/Pg extinction event, where smaller cryptic animals may have had greater chances of survival and subsequent diversification (Figure 4) (Longrich et al., 2012b; Klein, 2019). If true, then this has important implications for the debate on the origin of snakes, where miniaturized burrowers similar to blind snakes have been postulated to be ancestral to modern snakes, if not all snakes (e.g., Miralles et al., 2018). *Boipeba* suggests that the small body size of living blindsnakes does not characterize early blindsnakes, and cannot be extrapolated to early snakes in general.

Taken together, our findings provide a new perspective on the evolution of scolecophidians and early snakes. *Boipeba* provides evidence that blind snakes were already present and relatively large in the Mesozoic, and that the small size of living members of this group is likely due to subsequent miniaturization. Finally, the discovery of a scolecophidian in the Late Cretaceous of South America provides a crucial new calibration point for future molecular studies of divergence times within Serpentes.

Limitations of the Study

Our phylogenetic analyses robustly united *Boipeba* with living blind snakes (scolecophidians), but did not robustly resolve its placement within Scolecophidia. This is likely due to the limited number of informative phylogenetic characters that could be scored from vertebral characters alone. The lack of absolute dating of the minimum age of the fossil locality hampers a more precise estimate for the age of this fossil, which impacts the estimate of the size of the ancestral scolecophidian. However, our analyses consider the most conservative minimum age (66 Ma), which means the fossil could be much older and thus closer in time to the ancestral blind snake. This means that the large size of *Boipeba* would exert a stronger influence on the estimated size of the ancestral blind snake. Thus, a tighter (older) constraint on the minimum age of *Boipeba* would potentially improve support for the body size patterns retrieved here.

Resource Availability

Lead Contact

Further information and requests for resources and reagents should be directed to and will be fulfilled by the Lead Contact, Thiago Schineider Fachini (thiagoschineiderf@usp.br)

Materials Availability

The fossil is housed at the Museum of Palaeontology "Prof. Antônio Celso de Arruda Campos," Monte Alto, São Paulo State, Brazil. All the comparative material including fossils and extant specimens used for this study are housed at public institutions and thus accessible to scientists, and a list with all relevant specimens, CT scan imagery (including original slice data), and scripts for all phylogenetic and comparative analyses can be found in the Transparent Methods section in the supplemental file.

Data and Code Availability

All the relevant data for this study such as the used scripts for the phylogenetic analyses together with the unprocessed datasets, the surface reconstruction file, the supplementary figures in full resolution, and the raw CT-Scan slices are freely available at Mendeley Data repository (https://doi.org/10.17632/4dh8fj54f6.1). Original data have been deposited to Mendeley Data: [https://doi.org/10.17632/4dh8fj54f6.1].

METHODS

All methods can be found in the accompanying Transparent Methods supplemental file.

SUPPLEMENTAL INFORMATION

Supplemental Information can be found online at https://doi.org/10.1016/j.isci.2020.101834.

ACKNOWLEDGMENTS

We would like to thank Dr. Sandra Tavares (MPMA, Brazil) for allowing the access of the holotype for this study and Dr. Fabiano V. Iori (MPPC, Brazil) for fieldwork assistance and the preparation of the material. We want to thank the Willi Henning Society for free access to the software TNT. We also thank Daniel Cavalari (USP) for help with μCT. This study is part of the project "Core-facility for conservation of scientific documentation: biological collections and high technology research in comparative morphology" (CT-INFRA 01/2013), funded by Financiadora de Estudos e Projetos – FINEP, Ministry of Science, Technology, Innovation and Communication, Brazilian Federal Government. Funding was provided by Conselho Nacional de Desenvolvimento Científico e Tecnológico (CNPq Process nº 165031/2018-2) and Coordenação de Aperfeiçoamento de Pessoal de Nível Superior (CAPES) to T.S.F.; Fundação de Amparo à Pesquisa do Estado de São Paulo (FAPESP) under the main project "*Young Researchers Award*" led by A.S.H. (FAPESP Process n 2011/14080-0), and the Postdoctoral (2018/18145-9 to M.B) and Ph.D. grants (FAPESP Processes n 2017/00845-1 and 2019/11166-3) to S.O., Conselho Nacional de Desenvolvimento Científico e Tecnológico (CNPq Processes n 309434/2015-7 and 301014/2018-3) to A.S.H., and Australian Research Council grant DP200102328 to M.L. We also thank Dr. João Tonini for information on gene partitions in the DNA data from Tonini et al. (2016) and Professor Neusa Monteferrante for helping in the Latin etymology.

AUTHOR CONTRIBUTIONS

T.S.F. and A.S.H. conceived the project; T.S.F., S.O., A.P., and M.S.Y.L. wrote the manuscript with the input of the other authors; T.S.F. conducted the fieldwork and mechanically prepared, photographed, and CT-scanned the holotype; A.P. performed the size estimate of the fossil; A.P., T.S.F., and M.B. performed the digital preparation and segmentation of the specimen; S.O. and M.S.Y.L. prepared the figures; M.S.Y.L. and S.O. conducted the phylogenetic analyses; M.S.Y.L. performed the ancestral state reconstruction analyses; all authors analyzed, interpreted the data, and edited the final version of the manuscript.

DECLARATION OF INTERESTS

The authors declare no competing interests.

Received: July 31, 2020
Revised: September 4, 2020
Accepted: November 13, 2020
Published: December 18, 2020

REFERENCES

Albino, A., Carrillo-Briceño, J.D., and Neenan, J.M. (2016). An enigmatic aquatic snake from the Cenomanian of Northern South America. PeerJ *4*, e2027.

Augé, M., and Rage, J.C. (2006). Herpetofaunas from the upper Paleocene and lower Eocene of Morocco. Ann. Paléontol. *92*, 235–253.

Batezelli, A. (2017). Continental systems tracts of the Brazilian Cretaceous Bauru Basin and their relationship with the tectonic and climatic evolution of South America. Basin Res. *29*, 1–25.

Broadley, D.G., and Wallach, V. (2009). A review of the eastern and southern African blind-snakes (Serpentes: Typhlopidae), excluding Letheobia Cope, with the description of two new genera and a new species. Zootaxa *2255*, 1–100.

Burbrink, F.T., Grazziotin, F.G., Pyron, R.A., Cundall, D., Donnellan, S., Irish, F., Keogh, J.S., Kraus, F., Murphy, R.W., Noonan, B., et al. (2020). Interrogating genomic-scale data for Squamata (lizards, snakes, and amphisbaenians) shows no support for key traditional morphological relationships. Syst. Biol. *69*, 502–520.

Caldwell, M.W., Nydam, R.L., Palci, A., and Apesteguía, S. (2015). The oldest known snakes from the Middle Jurassic-Lower Cretaceous provide insights on snake evolution. Nat. Commun. *6*, 1–11, https://doi.org/10.1038/ncomms6996.

Caldwell, M.W., Reisz, R.R., Nydam, R.L., Palci, A. & Simões, T.R. (2016) *Tetrapodophis amplectus* (Crato Formation, Lower Cretaceous, Brazil) is not a snake. SVP Book of Abstracts. Society of Vertebrate Paleontology, Meeting program & Abstracts of the 76th Annual meeting, 108.

Caldwell, M.W. (2019). The Origins of Snakes: Morphology and Fossil Record (Taylor & Francis), p. 327.

Carvalho, I.D.S., De Vasconcellos, F.M., and Tavares, S.A.S. (2007). *Montealtosuchus arrudacamposi*, a new peirosaurid crocodile (Mesoeucrocodylia) from the late cretaceous Adamantina Formation of Brazil. Zootaxa *1607*, 35–46.

Castro, M.C., Goin, F.J., Ortiz-Jaureguizar, E., Vieytes, E.C., Tsukui, K., Ramezani, J., Batezelli, A., Marsola, J.C.A., and Langer, M.C. (2018). A Late Cretaceous mammal from Brazil and the first radioisotopic age for the Bauru Group. R. Soc. Open Sci. *5*, 180482.

Cundall, D., and Irish, F.J. (2008). The snake skull. In Biology of the Reptilia, the Skull of Lepidosauria, Volume 20, Morphology H, C. Gans, A.S. Gaunt, and K. Adler, eds. (Society for the Study of Amphibians and Reptiles)), pp. 349–692.

da Silva, Filipe, Fabre, Anne-Claire, Savriama, Yoland, Ollonen, Joni, Mahlow, Kristin, Herrel, Anthony, Müller, Johannes, and Di-Pöi, Nicolas (2018). The ecological origins of snakes as revealed by skull evolution. Nat. Commun. *9*, 1–11.

Dias-Brito, D., Musacchio, E.A., Castro, J.D., Maranhao, M.S., and Suárez, J.M. (2001). Grupo Bauru: uma unidade continental do Cretáceo no Brasil-concepções baseadas em dados micropaleontológicos, isotópicos e estratigráficos. Rev. Paléobiol. *20*, 245–304.

Feldman, A., Sabath, N., Pyron, R.A., Mayrose, I., and Meiri, S. (2016). Body sizes and diversification rates of lizards, snakes, amphisbaenians and the tuatara. Glob. Ecol. Biogeogr. *25*, 187–197.

Ferreira, G.S., Iori, F.V., Hermanson, G., and Langer, M.C. (2018). New turtle remains from the Late Cretaceous of Monte Alto-SP, Brazil, including cranial osteology, neuroanatomy and phylogenetic position of a new taxon. PalZ *92*, 481–498.

Figueroa, A., McKelvy, A.D., Grismer, L.L., Bell, C.D., and Lailvaux, S.P. (2016). A species-level phylogeny of extant snakes with description of a new colubrid subfamily and genus. PLoS One *11*, e0161070.

Garberoglio, F.F., Apesteguía, S., Simões, T.R., Palci, A., Gómez, R.O., Nydam, R.L., Larsson, H.C., Lee, M.S., and Caldwell, M.W. (2019a). New skulls and skeletons of the Cretaceous legged snake *Najash*, and the evolution of the modern snake body plan. Sci. Adv. *5*, eaax5833.

Garberoglio, F.F., Gómez, R.O., Apesteguía, S., Caldwell, M.W., Sánchez, M.L., and Veiga, G. (2019b). A new specimen with skull and vertebrae of *Najash rionegrina* (Lepidosauria: Ophidia) from the early Late Cretaceous of Patagonia. J. Syst. Palaeontol. *17*, 1533–1550.

Gobbo-Rodrigues, S.R., Petri, S., and Bertini, R.J. (1999). Ocorrências de ostrácodes na Formação Adamantina do Grupo Bauru, Cretáceo Superior da Bacia do Paraná e possibilidades de correlação com depósitos isócronos argentinos. Parte I–Família Ilyocyprididae. Acta Geol. Leopold. *23*, 3–13.

Goloboff, P.A., Farris, J.S., and Nixon, K.C. (2008). TNT, a free program for phylogenetic analysis. Cladistics *24*, 774–786.

Harrington, S.M., and Reeder, T.W. (2017). Phylogenetic inference and divergence dating of snakes using molecules, morphology and fossils: new insights into convergent evolution of feeding morphology and limb reduction. Biol. J. Linn. *121*, 379–394.

Hedges, S.B. (2008). At the lower size limit in snakes: two new species of threadsnakes (Squamata: Leptotyphlopidae: Leptotyphlops) from the Lesser Antilles. Zootaxa *1841*, 1–30.

Hsiang, A.Y., Field, D.J., Webster, T.H., Behlke, A.D., Davis, M.B., Racicot, R.A., and Gauthier, J.A. (2015). The origin of snakes: revealing the ecology, behavior, and evolutionary history of early snakes using genomics, phenomics, and the fossil record. BMC Evol. Biol. *15*, 1–87.

Hsiou, A.S., Albino, A.M., Medeiros, M.A., and Santos, R.A.B. (2014). The oldest Brazilian snakes from the early Late Cretaceous (Cenomanian). Acta Palaeontol. Pol. *59*, 635–642.

Iori, F.V., and de Souza Carvalho, I. (2009). *Morrinhosuchus luziae*, um novo Crocodylomorpha Notosuchia da Bacia Bauru, Brasil. Braz. J. Geol. *39*, 717–725.

Iori, F.V., and Carvalho, I.S. (2011). *Caipirasuchus paulistanus*, a new sphagesaurid (Crocodylomorpha, Mesoeucrocodylia) from the Adamantina Formation (upper cretaceous, Turonian–Santonian), Bauru Basin, Brazil. J. Vertebr. Paleontol. *31*, 1255–1264.

Iori, F.V., and Garcia, K.L. (2012). *Barreirosuchus franciscoi*, um novo Crocodylomorpha Trematochampsidae da Bacia Bauru, Brasil. Braz. J. Geol. *42*, 397–410.

Iori, F.V., Marinho, T.S., Carvalho, I.S., and Campos, A.A. (2013). Taxonomic reappraisal of the sphagesaurid crocodyliform *Sphagesaurus montealtensis* from the late cretaceous Adamantina Formation of São Paulo state, Brazil. Zootaxa *3686*, 183–200.

Iori, F.V., and Campos, A.C.D.A. (2017). Os Crocodiliformes da Formação Marília (Bacia Bauru, Cretáceo Superior) na Região de Monte Alto, estado de São Paulo, Brasil. Braz. J. Geol. *19*, 537–546.

Klein, C.G. (2019). Molecular and morphological patterns of survival, not extinction, of snakes through the Cretaceous-Paleogene mass extinction. Society of Vertebrate Paleontology, Meeting program & Abstracts of the 79th Annual meeting, 130.

Laduke, T.C., Krause, D.W., Scanlon, J.D., and Kley, N.J. (2010). A late cretaceous (Maastrichtian) snake assemblage from the Maevarano formation, Mahajanga basin, Madagascar. J. Vertebr. Paleontol. *30*, 109–138.

List, J.C. (1966). Comparative Osteology of the Snake Families Typhlopidae and Leptotyphlopidae, *vol. 36* (Illinois Biological Monographs).

Longrich, N.R., Bhullar, B.A.S., and Gauthier, J.A. (2012a). A transitional snake from the Late Cretaceous period of North America. Nature *488*, 205–208.

Longrich, N.R., Bhullar, B.A.S., and Gauthier, J.A. (2012b). Mass extinction of lizards and snakes at the Cretaceous–Paleogene boundary. Proc. Natl. Acad. Sci. U. S. A. *109*, 21396–21401.

Martill, D.M., Tischlinger, H., and Longrich, N.R. (2015). A four-legged snake from the early cretaceous of Gondwana. Science *349*, 416–419.

Mead, J.I. (2013). Scolecophidia (Serpentes) of the late Oligocene and early Miocene, North America, and a fossil history overview. Geobios *46*, 225–231.

Méndez, A.H., Novas, F.E., and Iori, F.V. (2014). New record of abelisauroid theropods from the Bauru group (upper cretaceous), São Paulo state, Brazil. Rev. Bras Paleontolog. *17*, 23–32.

Menegazzo, M.C., Catuneanu, O., and Chang, H.K. (2016). The South American retroarc foreland system: the development of the Bauru Basin in the back-bulge province. Mar. Petrol. Geol. *73*, 131–156.

Miralles, A., Marin, J., Markus, D., Herrel, A., Hedges, S.B., and Vidal, N. (2018). Molecular evidence for the paraphyly of Scolecophidia and its evolutionary implications. J. Evol. Biol. *31*, 1782–1793.

Onary, S., and Hsiou, A.S. (2018). Systematic revision of the early Miocene fossil *Pseudoepicrates* (Serpentes: Boidae): implications for the evolution and historical biogeography of the West Indian boid snakes (*Chilabothrus*). Zool. J. Linn. Soc. *184*, 453–470.

Paparella, I., Palci, A., Nicosia, U., and Caldwell, M.W. (2018). A new fossil marine lizard with soft tissues from the Late Cretaceous of southern Italy. R. Soc. Open Sci. *5*, 172411.

Pyron, R.A., and Wallach, V. (2014). Systematics of the blindsnakes (Serpentes: Scolecophidia: Typhlopoidea) based on molecular and morphological evidence. Zootaxa *3829*, 001–081.

Rage, J.C. (1984). Part 11 Serpentes. In Encyclopedia of Paleoherpetology, M. Wellnhofer, ed. (Gustav Fischer Verlag), pp. 1–79.

Ronquist, F., Teslenko, M., Van Der Mark, P., Ayres, D.L., Darling, A., Höhna, S.,., and Huelsenbeck, J.P. (2012). MrBayes 3.2: efficient Bayesian phylogenetic inference and model choice across a large model space. Syst. Biol. *61*, 539–542.

Santucci, R.M., and Arruda-Campos, A.D. (2011). A new sauropod (Macronaria, Titanosauria) from the Adamantina Formation, Bauru group, upper cretaceous of Brazil and the phylogenetic relationships of Aeolosaurini. Zootaxa *3085*, 1–33.

Singhal, S., Colston, T.J., Grundler, M.R., Smith, S.A., Costa, G.C., Colli, G.R., Moritz, C., Pyron, R.A., and Rabosky, D.L. (2020). Congruence and conflict in the higher-level phylogenetics of squamate reptiles: an expanded phylogenomic perspective. Syst. Biol. syaa054, https://doi.org/10.1093/sysbio/syaa054.

Swofford, D.L., and Sullivan, Jack (2003). PAUP: Phylogenetic Analysis Using Parsimony, version 4.0 b10. The Phylogenetic Handbook: A Practical Approach to DNA and Protein Phylogeny, *7* (Cambridge University Press), pp. 160–206.

Tavares, S.A.S., Branco, F.R., and Santucci, R.M. (2014). Theropod teeth from the Adamantina Formation (Bauru group, upper cretaceous), Monte Alto, São Paulo, Brazil. Cretac. Res. *50*, 59–71.

Tonini, J.F.R., Beard, K.H., Ferreira, R.B., Jetz, W., and Pyron, R.A. (2016). Fully-sampled phylogenies of squamates reveal evolutionary patterns in threat status. Biol. Conserv. *204*, 23–31.

Uetz, P., Freed, P., & Hošek, J. (2020). The reptile database http://www.reptiledatabase.org. Accessed 2.11.20.

Vidal, N., Marin, J., Morini, M., Donnellan, S., Branch, W.R., Thomas, R.,., and Hedges, S.B. (2010). Blindsnake evolutionary tree reveals long history on Gondwana. Biol. Lett. *6*, 558–561.

Xing, L., Caldwell, M.W., Chen, R., Nydam, R.L., Palci, A., Simões, T.R., McKellar, R.C., Lee, M.S.Y., and Wang, K. (2018). A mid-Cretaceous embryonic-to-neonate snake in amber from Myanmar. Sci. Adv. *4*, eaat5042.

Zaher, H., Apesteguia, S., and Scanferla, C.A. (2009). The anatomy of the upper cretaceous snake Najash rionegrina Apesteguía & Zaher, 2006, and the evolution of limblessness in snakes. Zool. J. Linn. Soc. *156*, 801–826.

Zheng, Y., and Wiens, J.J. (2016). Combining phylogenomic and supermatrix approaches, and a time-calibrated phylogeny for squamate reptiles (lizards and snakes) based on 52 genes and 4162 species. Mol. Phylogenet. Evol. *94*, 537–547.

iScience, Volume *23*

Supplemental Information

Cretaceous Blind Snake from Brazil Fills Major Gap in Snake Evolution

Thiago Schineider Fachini, Silvio Onary, Alessandro Palci, Michael S.Y. Lee, Mario Bronzati, and Annie Schmaltz Hsiou

Supplemental Information

Transparent Methods

Materials

The morphological comparative analyses were conducted after first-hand examination of specimens supplemented by relevant publications in the literature. Extant and fossil snakes, as well the accessed literature used for the description and comparative sections include "parviraptorids" (Caldwell et al., 2015); *Dinilysia patagonica* (MACN-RN unnumbered specimen) (Caldwell and Albino, 2003); *Najash* spp. (Garberoglio et al., 2019b; Zaher et al., 2009; Garberoglio et al., 2019a); "Madtsoiids" such as *Wonambi naracoortensis* (SAMA P16168), Pachyophiidae (Rage and Escuillié, 2000), *Coniophis precedens* (UALVP unnumbered specimen) (Longrich et al., 2012; Rage, 1984); *Boipeba tayasuensis* MPMA 16-0008-08; *Afrotyphlops punctatus* USNM 320704; *Afrotyphlops angolensis* AMNH 116633; *Typhlops jamaicensis* AMNH R160154; *Anilios (=Ramphotyphlops) pinguis* SAMA R924; *Ramphotyphlops polygrammicus* SAMA R3564; *Ramphotyphlops proximus* SAMA R915; *Ramphotyphlops ligatus* SAMA R2820; *Anilius scytale* AMNH R55613, AMNH R155256, MCZ 19537; *Cylindrophis ruffus* MNHN 1869 771, SAMA R36779; *Simalia (=Morelia) amethistina* SAMA R2605.

Institutional abbreviations

AMNH American Museum of Natural History, New York, USA.

MACN-RN Museo Argentino de Ciencias Naturales 'Bernardino Rivadavia', Buenos Aires, Argentina.

MPMA Museu de Paleontologia Prof. Antônio de Arruda Campos, São Paulo, Brazil.

MNHN Muséum national d'Histoire Naturelle, Paris, France.

MCZ Museum of Comparative Zoology, Cambridge, Massachusetts, USA.

USNM National Museum of Natural History, Washington, DC, USA.

SAMA R-REPTILES OR P-PALEONTOLOGY South Australian Museum of Adelaide, South Australia, Australia.

UALVP University of Alberta Laboratory for Vertebrate Paleontology, Edmonton, Alberta, Canada.

Methods

Anatomical nomenclature

Vertebral anatomical nomenclature for the description and comparisons follows Rage (1984); Auffenberg (1963); and Hoffstetter and Gasc (1969).

Phylogenetic analysis

To investigate the phylogenetic affinities of *Boipeba tayasuensis*, we added it to the data matrix derived from a recent study on snake evolution (Garberoglio et al., 2019a), along with four additional vertebral characters from Goméz et al. (2019) and one new (this study), resulting in dataset I - Morphology. A second dataset was built combining this morphological data matrix with the molecular data derived from a broad scale genomic study of squamates (Tonini et al., 2016), resulting in dataset II - Morphology plus DNA (See Supplementary data 3). These character-by-taxon matrices were assembled in the software Mesquite (Maddison and Maddison, 2019). Datasets I and II were each analysed using either all 37 taxa, or the 33 most complete taxa (taxa with >90% missing data were excluded). Analyses used both maximum parsimony and Bayesian Inference, resulting in eight analyses (see supplementary figures 3,4). The maximum parsimony analyses were performed using PAUP (Swofford, 2003), with *Varanus* as the outgroup, and among the 253 equally weighted morphological characters, 21 were multistate morphoclines and thus treated as ordered (data matrix in

transparent methods). The most parsimonious trees (MPTs) were inferred using Heuristic Search with 100 random addition sequence (RAS) replicates, and a strict consensus was obtained. Support values were calculated via TNT using the partitioned bootstrap (Siddal, 2010), with the morphology and DNA data resampled separately (supplementary figure 5). Bayesian inference analyses were performed in the software Mr. Bayes v 3.2.6 (Ronquist et al., 2012) employing the Mkv model (Lewis, 2001) with gamma rate variation for the morphological partition, while (for Dataset II) the DNA partitions and models were selected using PartitionFinder 2 (Lanfear et al., 2017). The analyses using dataset I (morphology only) were performed with four independent runs of 40 million generations, each run using 4 chains (1 heated and 3 cold), with the chains being sampled every 2000 generations, heating set to 0.06, and burn-in fraction of 25%. The analysis using dataset II (molecular + morphology) used similar settings, but with 12 chains per run (1 heated and 11 cold), temperature parameter set to 0.07, and burn-in fraction of 40%. The convergence in the posterior distribution was confirmed with high effective sample size (ESS > 200) for each parameter, potential scale reduction factors (PSRF) approaching 1, and the low standard deviation of split (clade) frequencies across runs (ASDSF < 0.01). Our analyses were not dated, but for visualization purposes the phylogenies were time-scaled in Fig. 4 using the stratigraphic ages of occurrence for the fossils and estimated divergence time dates derived from a recent phylogenomic study of squamates (Zheng and Wiens, 2016). Four additional phylogenetic analyses employing the same parameters were also conducted with the inclusion of the enigmatic taxon *Tetrapodophis amplectus* in the snake ingroup (supplementary figs. 6-8); the position of *Boipeba* within scolecophidians remains supported, but we are cautious not to overinterpret the topological results for *Tetrapodophis* due to its disputed ophidian affinities (Caldwell et al., 2016; Paparella et al. 2018; Caldwell, 2019). All the used scripts

and data matrix for the phylogenetic analyses can be freely downloaded at Mendeley Data Repository (doi: 10.17632/4dh8fj54f6.1).

Size estimate, snake body length plots and ancestral state reconstruction

The total length (TL) of *Boipeba tayasuensis* was estimated using the ratio between the average centrum length (CL) and total length including tail (TL) in four different taxa of extant typhlopoids, each represented by 1 specimen. We subdivided the trunk (precloacal) region of each specimen into five intervals of equal length, and sampled a trunk vertebra from each boundary between intervals (i.e. 4 trunk vertebrae per specimen). We measured the centrum length (along the ventral margin) of these 4 trunk vertebrae using a Zeiss microscope micrometer, and then calculated the average CL. We then calculated the ratio (R) between the TL of each of the four sampled specimens and its average trunk CL. These ratios produced four distinct TL estimates for *Boipeba* based on its CL (CL_b) (i.e. estimated TL of *Boipeba* = R x CL_b). We took the average of the four estimates as our conservative TL estimate of *Boipeba* (see supplementary data 1).

In order to compare the estimated body size of *Boipeba* with that of other extinct and extant snakes, we plotted histograms of the distribution of the TL of all living species of each terminal clade of snakes used in our snake phylogeny and the TL of important fossil snakes obtained from the literature (Fig. 4; "parviraptorids" were excluded due to the fragmentary nature of the fossils). The size data for extant taxa were obtained from a broad scale study of body size in lepidosaurs (Feldman et al., 2016), and plotted on a log scale using using R (R Core Team R, 2013); for details see supplementary data 2).

Ancestral state reconstructions for scolecophidian body size were performed using parsimony/likelihood methods. To infer the ancestral size of the MRCA of Scolecophidia, we took the tree from a dated, well-sampled squamate phylogeny (Zheng and Wiens, 2016),

retaining only the 98 blindsnake species for which TL size data was available (Feldman et al., 2016) and pruning other taxa (nexus file available at Mendeley Data Repository [doi: 10.17632/4dh8fj54f6.1]) . TL was scored (on a log scale) for all these species, and ancestral states for all nodes were estimated via Mesquite (Maddison and Maddison, 2019) using squared-changed parsimony accounting for branch lengths, which is identical to the maximum likelihood estimates under Brownian motion (Maddison, 1991). In order to observe the impact of the fossil when estimating the TL of the common ancestor of all blindsnakes (see supplementary figure 9), the first analysis was conducted exclusively using the 98 extant species, then a second analysis was performed adding *Boipeba* as sister group to Typhlopoidea (mid-way along the typhlopoid stem, and with tip age corresponding to a midpoint estimate of the stratigraphic age of the Adamantina Formation; i.e. 76.85 Ma (87.78-66Ma).

CT scanning and image segmentation

High-resolution microCT scanning of *Boipeba tayasuensis* was conducted using a GE Phoenix v|tome|x S240 scanner at the Centro para Documentação da Biodiversidade, Departamento de Biologia (Universidade de São Paulo, Ribeirão Preto, Brazil). The virtual preparation and segmentation procedure were conducted in the software AVIZO lite v. 9.0, initially employing the threshold tool to remove the rock matrix, followed by manual slice-by-slice segmentation (in the three-axis view) using the brush and lasso tools. The segmented vertebra was then rendered as a surface file (.stl) for three-dimensional visualization. The raw CT-scan files together with the.stl file are available at Mendeley Data Repository (doi: 10.17632/4dh8fj54f6.1).

Systematic palaeontology of indeterminate ophidian material

Three articulated ophidian vertebrae were discovered in close proximity to the holotype of *Boipeba tayasuensis*. Despite the close association, a detailed comparison of the type material of *B. tayasuensis* with the other vertebrae does not support their assignment to the same taxon. (see below).

Systematic Palaeontology

Squamata Oppel, 1811

Ophidia Brongniart, 1800

Genus and species indet.

(Figure S10)

Material. Sequence of three fragmentary vertebrae (unregistered specimen).

Locality and horizon. Same from the type locality of *Boipeba tayasuensis*.

Description. The material comprises a series of three poorly preserved articulated ophidian vertebrae. The vertebrae can be confidently assigned to Ophidia due to the presence of well-developed zygosphenes and zygantra, and synapophyses subdivided into ventral and dorsal articulatory facets. The general morphology of the vertebrae is quite distinct when compared to *Boipeba* in having: higher neural spines; a concave anterior margin of the zygosphene roof; less depressed neural arch; trefoil-shaped cross section of the neural canal; the absence of prezygapophyseal processes; and a strong differentiation between ventral and dorsal articular facets of the synapophyses, with a convex diapophyseal articular facet and a subtriangular parapophyseal articular facet. The latter is ventrally oriented, and extends below the ventral margin of the cotyle. The synapophysis morphology is sharply distinct from the condition in *Boipeba*, which possesses a confluent (i.e. not divided) synapophysis. Due to poor preservation

and lack of diagnostic features, the taxonomic assignment of this material is hampered. Some features such as the absence of prezygapophyseal articular processes and the slightly concave anterior edge of the zygosphene (heart-shaped morphology) are also present but not exclusive to "madtsoiids". The presence of distinct articular facets of the synapophyses is a feature widely distributed among extinct and extant snakes (with exception of *Boipeba* and scolecophidians). Given the morphological differences between *Boipeba* and the articulated series together with the lack of diagnostic morphological features, here we retain the conservative approach of identifying the material as indeterminate ophidian. The likely presence of a distinct indeterminate ophidian taxon co-occurring with *Boipeba* reinforces the underestimated snake fossil diversity of the Cretaceous of the Bauru Basin, which, aside from *Boipeba*, currently includes only two other non-described snake taxa (Onary et al., 2017). Only additional findings will help elucidate the taxonomic affinities of this fragmentary fossil snake.

About the raw data files

All the relevant data for this study such as the used scripts for the phylogenetic analyses together with the unprocessed datasets, the surface reconstruction file, the supplementary figures in full resolution and the raw CT-Scan slices are freely available at Mendeley Data repository (doi: 10.17632/4dh8fj54f6.1).

Character list used for the phylogenetic analyses

For the phylogenetics analyses we used the character list derived from Garberoglio et al., (2019b), along with four additional vertebral characters from Goméz et al., 2019 (249, 250, 252, 253) and one new (251). The following 21 characters were multistate morphoclines and thus treated as ordered: 13, 25, 44, 46, 56, 62, 78, 94, 108, 114, 117, 119, 128, 140, 167, 207, 225, 229, 234, 250, 253. Numbering of characters 1-248 follows Garberoglio et al., (2019a)

DENTITION

1. Maxillary and dentary teeth: relatively short conical, upright (0); robust, recurved (1); elongate needle-shaped, distinctly recurved (2).
2. Premaxillary dentition: present (0); absent (1).
3. Alveoli and base of teeth: not expanded transversely (0); wider transversely than anteroposteriorly (1).
4. Pterygoid teeth: absent (0); present (1).

SKULL

5. Premaxilla: broadly articulated with maxilla (0); loosely contacting maxilla (1).
6. Transverse processes of premaxilla: curved backwards (0); extending straight laterally or anterolaterally (1).
7. Nasal process of premaxilla: elongate, approaching or contacting frontals (0); short, divide nasals only at anterior margin or not at all (1).
8. Dorsal (horizontal) lamina of nasal: relatively broad anteriorly, with narrow gap between lateral margin and vertical flange of septomaxilla (0); dorsal lamina of nasal distinctly tapering anteriorly, leaving wide gap between lateral margin and vertical flange of septomaxilla (1).
9. Medial flanges of nasal, articulation with median frontal pillars: present (0); absent (1)
10. Anterior margin of nasals: restricted to posteromedial margins of nares (0); extend anteriorly toward tip of rostrum (1).
11. Lateral flanges of nasals: articulate with anterior margin of frontals (0); separated from frontals (1).
12. Posterolateral margin of nasal: contacts anteromedian margin of prefrontal (0); elements in contact along most of their length (1); contact between elements with interfingering of nasal and prefrontal margins (2); nasals do not contact prefrontals (3).
13. Septomaxilla posterior dorsal process of lateral vertical flange: absent (0); short (1); long (2).
14. Septomaxilla articulation with median frontal pillars: absent (0); present (1).
15. Ventral portion of posterior edge of lateral flange of septomaxilla and opening of Jacobsen'sorgan: located at level of posterior edge or behind (0); distinctly in front (1).
16. Vomeronasal cupola: fenestrated medially (0); closed medially by a sutural contact of septomaxilla and vomer (1).
17. Septomaxilla: forms lateral margin of opening of Jacobson's organ (0); vomer extends into posterior part of lateral margin, restricting septomaxilla to anterolateral part of lateral margin of opening of Jacobson's organ (1).
18. Vomeronasal nerve: does not pierce vomer (0); exits vomer through single large foramen (1); through cluster of small foramina (2).
19. Posterior ventral (horizontal) lamina of vomer: long, parallel edged (0); short, tapering to pointed tip (1).
20. Posterior dorsal (vertical) lamina of vomer: well developed (0); reduced or absent (1).

21. Prefrontal: articulates with frontal laterally (0); anterolaterally (1).
22. Lateral margin of prefrontal: slanting anteroventrally (0); positioned vertically (1).
23. Lacrimal foramen on prefrontal: not completely enclosed (0); enclosed by prefrontal (1); prefrontal lacking foramen (2).
24. Lateral foot process of prefrontal: absent (0); contacts maxilla only (1); maxilla and palatine (2); palatine only (3).
25. Medial foot process of prefrontal: absent (0); present, low (1); present, high (2).
26. Anterior/lateral flange of prefrontal covering nasal gland and roofing auditus conchae: absent (0); present (1).
27.Ventral margin of lateral surface of prefrontal: articulates with dorsal surface of maxilla (0); retains only posterior contact (1).
28. Dorsal lamina of prefrontal: contacts or forms overlapping contact with nasal posteromedially (0); remains separate from nasal (1).
29. Medial frontal pillars: absent (0); present (1).
30. Transverse horizontal shelf of frontal: developed and broadly overlapped by nasals (0); poorly developed and never broadly overlapped by nasals (1); absent (2).
31. Lacrimal: present (0); absent (1).
32. Postfrontal: present (0); absent (1).
33. Jugal: present (0); fused or absent (1).
34.Jugal, ventral tip: Contact or approaches prefrontal (or lacrimal), forming or contributing to ventral margin of orbit (0); contacts or closely approaches ectopterygoid/maxilla, forming almost complete posterior margin of orbit (1); remains separated by wide gap from ectopterygoid (2).
35.Jugal, dorsal head: contacts postorbital (0); contacts parietal (1); fuses or articulates with only the posterodorsal surface of postfrontal (2); lack of dorsal contact (3).
36. Parietal: without lateral wings meeting postorbital bones (0); with lateral wings meeting postorbital bones (1).
37. Distinct lateral ridge of parietal: extending posteriorly from anterior lateral wing up to prootic: absent (0); present (1).
38. Frontoparietal suture: relatively straight (0); frontoparietal suture U-shaped (1).
39. Optic foramen, posterior margin: posteriorly located, straight parietal margin (0), posteriorly located, concave parietal margin (1); anteriorly located, posterior border within frontal (2).
40. Lateral margins of braincase open anterior to prootic (0); descending lateral processes of parietal enclose braincase (1).
41. Supratemporal processes of parietal: distinctly developed (0); not distinctly developed (1).
42. Parietal enters anterior aspect of base of basipterygoid process: absent (0); present (1).
43. Contact between parietal and supraoccipital: V-shaped with apex pointing anteriorly (0); straight transverse line (1); V-shaped with apex pointing posteriorly (2).
44. Ascending process of maxilla: tall, extending to dorsal margin of prefrontal (0); short (1); absent (2).
45. Small horizontal shelf on medial surface of anterior end of maxilla: present (0); absent (1).
46. Posterior end of maxilla: does not project beyond posterior margin of orbit (0); projects moderately beyond posterior margin of orbit (1); projects distinctly beyond posterior margin of orbit, with broad flat surface (2).
47. Medial (palatine) process of maxilla: located in front of orbit (0); located below orbit (1).
48. Medial (palatine) process of maxilla: pierced (0); not pierced (1).
49. Anterior end of supratemporal: located behind or above posterior border of trigeminal

foramen (0); anterior to posterior border of trigeminal foramen (1).
50. Supratemporal facet on opisthotic-exoccipital: flat (0); sculptured and delineated with projecting posterior rim that overhangs exoccipital (1).
51. Free-ending posterior process of supratemporal: absent (0); present (1).
52. Supratemporal: present (0); absent (1).
53. Anterior dentigerous process of palatine: absent (0); present (1).
54. Medial (choanal) process of palatine: forms extensive concave surface dorsal to ductus nasopharyngeus (0); narrows abruptly to form curved finger-like process (1); forms short horizontal lamina that does not reach vomer (2).
55. Choanal process of palatine: without expanded anterior flange articulating with vomer (0); with anterior flange (1).
56. Pterygoid contacts palatine: complex and finger-like articulations (0); tongue-in-groove joint (1); reduced to flap-overlap (2).
57. Palatine contact with ectopterygoid: present (0); absent (1).
58. Dentigerous process of palatine contact with vomer and/or septomaxilla posterolateral to opening for Jacobson's organ: present (0); absent (1).
59. Maxillary process of palatine: anterior to posterior end of palatine (0); at posterior end of palatine (1).
60. Lateral (maxillary) process of palatine and maxilla: in well-defined articulation (0); loosely overlapping medial (palatine) process of maxilla, or absent (1).
61. Maxillary branch of trigeminal nerve: pierces lateral (maxillary) process of palatine (0); passes dorsally between palatine and prefrontal (1).
62. Vomerine (choanal) process of palatine: articulates broadly with posterior end of vomer (0); meets vomer in well-defined articular facet (1); touches or abuts vomer without articulation or remains separated from vomer (2).
63. Internal articulation of palatine with pterygoid: short (0); long (1).
64. Pterygoid tooth row: anterior to basipterygoid joint (0); tooth row reaches or passes level of basipterygoid joint (1).
65. Quadrate ramus of pterygoid: robust, rounded or triangular in cross-section, but without groove (0): blade-like and with distinct longitudinal groove for protractor pterygoidei (1).
66. Transverse (lateral) process of pterygoid: forms distinct, well-defined lateral projection (0); gently curved lateral expansion of pterygoid, or absent (1).
67. Lateral edge of ectopterygoid: straight (0); angulated at contact with maxilla (1).
68. Anterior end of ectopterygoid: restricted to posteromedial edge of maxilla (0); invades dorsal surface of maxilla (1).
69. Pterygoid attached to basicranium: by strong ligaments at palatobasal articulation (0); pterygoid free from basicranium in dried skulls (1).
70. Quadrate: slender (0); broad (1).
71. Quadrate: slanted clearly anteriorly, posterior tip of pterygoid dislocated anteriorly from mandibular condyle of quadrate (0); positioned slight anteriorly or vertically (cephalic condyle positioned behind or at same level of mandibular condyle) (1); slanted posteriorly (cephalic condyle positioned in front of mandibular condyle) (2).
72. Cephalic condyle of quadrate: elaborated into posteriorly projecting suprastapedial process (0); suprastapedial process absent or vestigial (1).
73. Stapedial footplate: broad and massive (0); narrow and thin (1).
74. Stylohyal: not fused to quadrate (0); fuses to posterior tip of suprastapedial process (1); fusesto ventral aspect of reduced suprastapedial process (2); stylohyal fuses to quadrate shaft (3).
75. Stapedial shaft: straight (0); angulated (1).
76. Stapedial shaft: slender and longer than diameter of stapedial foot-plate (0); thick, and

equal to, or shorter than diameter of stapedial footplate (1).
77. Paroccipital process of otooccipital: well developed and laterally projected (0); reduced to short projection or absent (1).
78. Juxtastapedial space defined by a crista prootica, crista tuberalis and crista interfenestralis: absent (0); present, but not completely enclosed ("incipient"crista circumfenestralis) (1); present and enclosed (i.e., fully developed crista circumfenestralis) (2).
79. Stapedial footplate: mostly exposed laterally (0); Prootic and otoocipital converges upon stapedial footplate (1).
80. Crista interfenestralis: does not form individualized component around the juxtastapedial space (0); does form individualized component around juxtastapedial space (1).
81. Jugular foramen: exposed in lateral view by crista tuberalis (0); concealed in lateral view by crista tuberalis (1).
82. Otooccipitals: do not contact each other dorsally (0); contact each other dorsally (1).
83. Basioccipital posterolateral processes: short and narrow, do not extend toward posterior margin of occipital condyle (0); wider than condyle and long, combine with crista tuberalis to extend to approximate posterior margin of occipital condyle (1).
84. Supraoccipital contact with prootic: narrow (0); broad (1).
85. Prootic exclusion of parietal from trigeminal foramen: absent (0); present (1).
86. Laterosphenoid: absent (0): present (1).
87. Prootic ledge underlap of posterior trigeminal foramen: absent (0); present (1).
88. Prootic: exposed in dorsal view medial to supratemporal or to supratemporal process of parietal (0); fully concealed by supratemporal or parietal in dorsal view (1).
89. Exit hyomandibular branch of facial nerve inside opening for mandibular branch of trigeminal nerve: absent (0); present (1).
90. Vidian canal: does not open intracranially (0); open intracranially (1).
91. Anterior opening of Vidian canal: single (0); divided (1).
92. Sella turcica: bordered posteriorly by well-developed dorsum sellae (0); dorsum sellae low (1); dorsum sellae not developed, sella turcica with shallow posterior margin (2).
93. 'Lateral wings of basisphenoid': absent (0); present (1).
94. Ventral surface of basisphenoid: smooth (0); with weakly developed sagittal crest from which protractor pterygoidei originates (1); with strongly projecting sagittal crest (2).
95. Basioccipital: contributes to ventral margin of foramen magnum (0); basioccipital excluded by medial contact of otooccipitals (1).
96. Basisphenoid-basioccipital suture: smooth (0); transversely crested (1).
97. Basipterygoid (= basitrabecular) processes: present (0); absent (1).
98. Crista trabeculares: short and or indistinct (0); elongate and distinct in lateral view (1).
99. Cultriform process of parabasisphenoid: does not extend anteriorly to approach posteriormargin of choanae (0); approaches posterior margin of vomer (1).
100. Parabasisphenoidal rostrum behind optic foramen: narrow (0); broad (1).
101. Parabasisphenoid rostroventral surface: flat or broadly convex (0); concave (1).
102. Basioccipital meets parabasisphenoid: suture located at level of fenestra ovalis (0); located at or behind trigeminal foramen (1); basioccipital and parabasisphenoid fused (2).
103. Parasphenoid rostrum interchoanal process: absent (0); broad (1); narrow (2).

MANDIBLE
104. Anteromedial margin of dentaries: symphyseal articular facet (0); no symphyseal facet (1).
105. Posterior dentigerous process of dentary: absent (0); present, short (1); present, long (2).
106. Medial margin of adductor fossa: relatively low and smoothly rounded (0); forms

distinct dorsally projecting crest (1).
107. Mental foramina on lateral surface of dentary: two or more (0); one (1).
108. Coronoid process of coronoid bone: high, tapering distally (0); high, with rectangular shape (1); low, not exceeding significantly coronoid process of compound bone (2).
109. Coronoid bone: present (0); absent (1).
110. Posteroventral process of coronoid: present (0); absent (1).
111. Coronoid process on lower jaw: formed by coronoid bone only (0); or by coronoid and compound bone (1); or by compound bone only (i.e. coronoid absent) (2).
112. Posdentary elements: presence of separate elements (0); fusion of surangular /articular intocompound bone (1).

VERTEBRAE
113. Chevrons: present (0); absent (1).
114. Hemapophyses: absent (0); present, short (1); present, long (2).
115. Hypapophyses: restricted to anterior-most precloacal vertebrae (0); present throughout precloacal skeleton (1).
116. Para-diapophysis: confluent (0); separated into dorsal and ventral facet (1).
117. Prezygapophyseal accessory processes: absent (0); present, short (1); present, long
118. Subcentral paralymphatic fossae on posterior precloacal vertebrae: absent (0); present (1).
119. Subcentral foramina: absent (0); present, consistently small (1); present, of variable size (2).
120. Well-developed, consistently distributed paracotylar foramina: absent (0); present (1).
121. Ventral margin of centra: smooth (0); median prominence from cotyle to condyle (1).
122. Axis intercentrum: not fused to anterior region of axis centrum (0); fused (1).
123. Neural spine height: well-developed process (0); low ridge or absent (1).
124. Posterior margin of neural arch: shallowly concave in dorsal view (0); with deep V-shaped embayment in dorsal view (1).
125. Cotyle shape of precloacal vertebrae: oval (0); circular (1).
126. Parazygantral foramen: absent (0); present (1).
127. Lymphapophyses: absent (0); present (1).
128. Lymphapophyses: three or fewer (0); three lymphapophyses and one forked rib (1); more than three lymphapophyses and one forked rib (2).
129. Sacral vertebrae: present (0); absent (1).
130. Position of synapophyses in relation to lateral edge of prezygapophyses: at same level or slightly more projected laterally (0); clearly medial to edge of prezygapophyses (1).
131. Pachyostotic vertebrae: absent (0); present (1).
132. Precloacal vertebrae number: fewer than 100 (0); more than 100 (1).
133. Caudal vertebrae number: greater than 50% of precloacal number (0); approximately 10% or less than precloacal number (1).
134. Tuber costae absent from ribs (0), tuber costae present (1).

HINDLIMBS
135. Pectoral girdle and forelimbs: present (0); absent (1).
136. Tibia, fibula, and hind foot: present (0); absent (1).
137. Trochanter externus: present (0); absent (1).
138. Pelvis: external to sacral-cloacal ribs (0); internal to sacral-cloacal ribs (1).
139. Ilium and pubis length: ilium longer than pubis (0); ilium and pubis of same size (1); pubis much longer than ilium (2).
140. Pelvic elements: with strongly sutured contact (0); with weak (cartilaginous) contact (1);

fused together (2).
141. Pelvic elements: present (0); absent (1).
142. Medial vertical flanges of nasals: absent (0); present (1).
143. Preorbital ridge: dorsally exposed (0); overlapped by prefrontal (1).
144. Lateral foot process of prefrontal: articulates with lateral edge of maxilla via thin anteroposteriorly directed lamina (0); articulates with maxilla via large contact that runs from lateral to medial dorsal surface of maxilla (1).
145. Medial finger-like process of ectopterygoid articulating with medial surface of maxilla:present (0); absent (1).
146. Posterolateral corners of basisphenoid: strongly ventrolaterally projected (0); not projected (1).
147. Basioccipital: expanded laterally to form floor of recessusscalae tympani (0); excluded from floor of recessusscalae tympani by otooccipital (1).
148. Frontal subolfactory process: absent or present as simple horizontal lamina (0); present and closing tractus olfactorius medially (1).
149. Ectopterygoid contact with pterygoid: restricted to transverse (lateral) process of pterygoid (0); contact expanded significantly on dorsal surface of pterygoid body (1).
150. Maxillary process of palatine: main element bridging contact with maxilla and palatine inventral view (0); covered ventrally by expanded palatine process of maxilla (1).
151. Coronoid bone contributes to anterior margin of adductor fossa: present (0); absent (1).
152. Coronoid bone: sits mostly on dorsal and dorsomedial surfaces of compound bone, being exposed in both lateral and medial views of mandible (0); applied to medial surface of compound bone (1).

TEETH
153. Teeth, implantation: interdental ridges absent (0): interdental ridges present (1).
154. Teeth, replacement: replacement teeth lie vertically (0); lie horizontally in jaws (1).
155. Teeth, replacement: single replacement tooth per tooth position (0); two or more replacement teeth per tooth position (1).
156. Teeth, attachment: ankylosed to jaws (0); teeth loosely attached by connective tissue (1).
157. Teeth, size: crowns isodont or enlarged at middle of tooth row (0) crowns large anteriorly,and decrease in size posteriorly (1); anterior teeth conspicuously elongate, length of crown significantly exceeds height of dentary at midlength (2).

SKULL
158. Premaxilla: ascending process transversely expanded, partly roofing external nares (0); ascending process mediolaterally compressed, blade-like or spine-like (1).
159. Premaxilla: premaxilla medial to maxillae (0); located anterior to maxillae (1).
160. Prefrontal: prefrontal socket for dorsal peg of maxilla absent (0); present (1).
161. Prefrontal extends medially across frontal for more than 75% of width of frontal: absent (0); present (1).
162. Expanded naris: Weakly developed naris (0); strongly concave anterior margin of prefrontal bordering naris (1).
163. Frontal: nasal processes of frontal project between nasals (0); nasal processes absent (1).
164. Frontals: frontals taper anteriorly, distinct interorbital constriction (0); frontals broad anteriorly, interorbital region broad (1).
165. Frontal: subolfactory process abuts prefrontal in immobile articulation (0); subolfactory process articulates with prefrontal in mobile joint (1); subolfactory process with distinct lateral peg or process that clasped dorsally and ventrally by prefrontal (2).
166. Frontals and parietals: do not contact ventrally (0); descending wings of frontals and

parietals contact ventrally to enclose optic foramen (1).
167. Parietal, sagittal crest: absent (0); present posteriorly but not anteriorly, and extending for no more than 50% of parietal midline length (1); present anteriorly and posteriorly, and extending more than 50% of parietal midline length (2).
168. Parietal: narrow (0); inflated (1).
169. Parietal. Posteriorly broad parietal (0); posteriorly narrow parietal (1)
170. Skull, postorbital region relative length: short, less than half (0); elongate, half or more (1).
171. Supraoccipital region of skull: nuchal crests absent (0); present (1).
172. Supratemporal: supratemporal short, does not extend posterior to paroccipital process (0); elongate, extending well beyond paroccipital process (1).
173. Maxilla: palatine process short, weakly developed (0); palatine process long, strongly projecting medially (1).
174. Maxilla, premaxillary process: medial projection articulating with vomers present (0); premaxillary process does not contact vomers (1).
175. Maxilla, number of mental foramina: 5 or more (0); 4 or fewer (1).
176. Maxilla, supradental shelf development: extending full length of maxilla (0); reduced anterior to palatine process (1).
177. Maxilla, medial surface of facial process with distinct naso-lacrimal recess demarcated dorsally by anteroventrally trending ridge: present (0); absent (1).
178. Maxilla, medial surface of facial process with well-defined fossa for lateral recess of nasal capsule: present (0); reduced and present as small fossa on back of facial process (1); absent, fossa for lateral recess developed entirely on prefrontal (2).
179. Maxilla: extensive contact of dorsal margin of maxilla with nasal (0); nasal-maxilla contact lost (1).
180. Maxilla: maxilla overlaps prefrontal laterally in tight sutural connection (0); overlap reduced, mobile articulation (1).
181. Maxilla: palatine process of maxilla projects medially (0); palatine process of maxilla downturned (1).
182. Maxilla, superior alveolar foramen: positioned near middle of palatine process, opening posterodorsally (0); positioned near anterior margin of palatine process, opening medially (1).
183. Maxilla, accessory foramen posterior to palatine process: absent (0); present (1).
184. Maxilla, ectopterygoid process: absent (0); present (1).
185. Maxilla: 15 or more maxillary teeth (0); fewer than 15 maxillary teeth (1); maxilla without teeth (2).
186. Postfrontal: anterior and posterior processes clasping frontals and parietals (0); anterior and posterior processes present, but postfrontal abuts frontals and parietals (1); anterior and posterior processes absent (2).
187. Supratemporal: free caudal end of supratemporal projects posteroventrally (0); posteriorly or posterodorsally (1).
188. Quadrate, lateral conch: present (0); absent (1).
189. Quadrate, maximum length relative to proximal width: quadrate elongate, maximum length at least 125% of maximum width of quadrate head (0); quadrate short, length less than 125% of width of quadrate head (1).
190. Quadrate, proximal end plate-like: absent (0); present (1).
191. Palatine, dentition: teeth small relative to lateral teeth (0); enlarged, palatine teeth at least half diameter of posterior maxillary teeth (1); palatine lacking dentition (2).
192. Palatine, elongate lateral process projecting to lateral edge of orbit to articulate with caudal margin of prefrontal: absent (0); present (1).
193. Epipterygoid: present (0); absent (1).

194. Ectopterygoid: clasps pterygoid anteromedially (0); ectopterygoid overlaps pterygoid (1); ectopterygoid abuts pterygoid medially (2).
195. Vidian canals: posterior openings symmetrical (0); asymmetrical (1).
196. Exoccipital-opisthotic: horizontal, wing-like crista tuberalis absent (0); present (1).
197. Otooccipitals: do not project posteriorly to level of occipital condyle (0); project posteriorly to conceal occipital condyle in dorsal view (1).
198. Sclerotic ring: present (0); absent (1).

MANDIBLE
199. Dentary, enlarged mental foramen: absent (0); present (1).
200. Dentary, depth of Meckelian groove anteriorly: deep slot (0); shallow sulcus (1).
201. Dentary, angular process shape: posteroventral margin of dentary angular process weakly wrapped around underside of jaw (0); dentary angular process projects more nearly horizontally to wrap beneath jaw (1).
202. Dentary, angular process length relative to coronoid process: angular process distinctly shorter than coronoid process, former terminating well anterior to latter (0); subequal in length posteriorly (1).
203. Dentary, symphysis: weakly projecting medially (0); hooked inward and strongly projecting medially (1).
204. Dentary, ventral margin: unexpanded, medial margin of dentary straight in ventral view (0); expanded, medial margin crescentic in ventral view (1).
205. Dentary, coronoid process: wraps around surangular laterally and medially (0); broad and sits atop surangular (1).
206. Dentary, coronoid process with slot for medial tab of surangular: absent (0) or present (1).
207. Dentary, subdental shelf: present along entire tooth row (0); present only along posterior portion of tooth row (1); absent (2).
208. Surangular, dentary process with distinct triradiate cross-section: absent (0); present (1).
209. Surangular, adductor fossa: small or absent (0); extended caudally towards jaw articulation (1).
210. Surangular: ventrolateral surface of surangular bearing distinct crest for attachment of adductor muscles: absent (0); present (1).
211. Coronoid, lateral overlap of coronoid onto dentary: absent (0); present (1).
212. Splenial attachment to dentary above Meckel's canal: close throughout length (0); loose,with dorsal dentary suture confined to posterodorsal corner of splenial (1); contact with subdental shelf reduced to small spur of bone or contact lost entirely (2).
213. Splenial - angular articulation: splenial overlaps angular (0); splenial abuts against angular to form hinge joint (1).
214. Splenial, size: splenial elongate, extends more than half distance from angular to dentary symphysis (0); splenial short, extends less than half distance from angular to symphysis (1).
215. Splenial, anterior mylohyoid foramen: present (0); absent (1).
216. Angular, lateral exposure (with coronoid region pointing dorsally): angular broadly exposed laterally along length (0); angular narrowly exposed laterally (1).
217. Angular, length posteriorly relative to glenoid (quadrate articulation): relatively long,extends more than half distance from anterior end of angular to glenoid; (0) relatively short,half or less of distance to glenoid (1); very short, one third or less of distance to glenoid (2).
218. Surangular, enlarged anterior surangular foramen: absent (0); or present (1).
219. Coronoid eminence: well-developed (0); weakly developed or absent (1).

220. Glenoid, shape: quadrate cotyle shallow (0), anteroposteriorly concave and transversely arched, ‘saddle shaped’ (1).
221. Retroarticular process: retroarticular process elongate (0) or shortened (1).
222. Hypapophyses of anterior precloacals: short, about 50% length of centrum (0); long, subequal to or longer than centrum (1).
223. Vertebrae, ridge-like or bladelike ventral keels developed posterior to hypapophyses: absent (0); present (1).
224. Vertebrae, dorsolateral ridges of neural arch: absent (0); present (1).
225. Vertebrae, vertebral centrum: narrow in ventral view (0); broad and subtriangular in shape (1); broad and square (2).
226. Vertebrae, arterial grooves: absent in neural arch (0); present (1).
227. Vertebrae, posterior condyle: confluent with centrum ventrally (0); distinctly separated from centrum by groove/constriction between centrum and condyle (1).
228. Vertebrae: narrow, width across zygapophyses not significantly greater than distance from prezygapophyses to postzygapophyses (0); vertebrae wide, width across zygapophyses 150% of length or more (1).
229. Vertebrae, zygosphene anterior margin: deeply concave anterior edge (0); shallowly concave anterior edge (1); straight or slightly sinuous anterior edge (2).
230. Basioccipital, ventral surface: smooth (0); sagittal crest of parabasisphenoid extends into basiocciptal (1).
231. Vertebrae, zygosphene width, expressed as ratio of zygosphene width to cotyle width, in anterior view: wide, ratio close to or more than 1 (0); narrow, ratio significantly less than 1 (1).
232. Vertebrae, constriction index, expressed as neural arch minimal width to total width, measured at the level of the prezygapophyseal lateral edge: slight constriction, ratio equal to or more than 0.67 (0); marked constriction, ratio less than 0.67 (1).
233. Vertebrae, narrow and sharp haemal keel: absent (0); present (1).
234. Vertebrae, cotyle size, expressed as ratio of cotyle width to total width (measured as the interdiapophyseal width): big cotyle, ratio more than 0.5 (0); middle-sized cotyle, ratio between 0.5 and 0.3 (1); small cotyle, ratio less than 0.3 (2).
235. Vertebrae, small lateral ridge on precloacal vertebrae extending from the parapophyses, below lateral foramen: absent (0); present (1).
236. Supraoccipital, shape of dorsal exposure: broad and square (0); wider than longer, with broad edges (rectangular) (1); wider than long, with pointed medial edges (2); diamond-shaped (3); ‘M’-shaped (4); absent or fused (5).
237. Supraoccipital, size of dorsal exposure, expressed as ratio of supraoccipital length (measured at the midline) to parietal width (measured at the line delimited by the anterior borders of the prootic): big, ratio of 0.5 or more (0); small, ratio clearly less than 0.5 (1).
238. Vertebrae: unfused intercentra in precloacal vertebrae posterior to the axis, present (0); absent (1).
239. Jugal, distinct posterior process for quadratomaxillary ligament: present (0); absent (1).
240. Postorbital: present (0); absent (1)
241. Vertebrae, arqual ridges on middle precloacals: absent (0); present (1)
242. Pubis, obturator foramen: present (0); absent (1).
243. Ascending/facial process of maxilla, posterior notch on medial surface for prefrontal: present (0); absent (1).
244. Dentition, dentary teeth: present (0); absent (1).
245. Parietals: single (0); remain paired in adult skull (1)
246. Supraoccpitals: single (0); remain paired in adult skull (1)
247. Prootic: separated element (0); fused to braincase (1)

248. Ectopterygoid: present (0); highly reduced or absent (1).
249.Parapophysis ventral margin: high, placed dorsal to the ventral margin of cotyle (0); ventrally projected, level with or below ventral margin of cotyle (1).
250. Absolute size of neural spine, expressed as neural spine height (measured from dorsal edge of zygosphene) to total height of vertebra: high, >30% (0); moderate, between 15-30% (1); low, less than 15% (2).
251.Neural arch morphology flattened, dorsoventrally compressed (0); dorsoventrally expanded, vaulted (1).
252.Condyles of middle precloacal verterbrae, orientation: facing very dorsally, ventral edge (at most) of condyle surface exposed in ventral view (0); facing posteriorly, or posterodorsally, much of condyle surface exposed in ventral view (1).
253. Orientation of zygapophyses of middle precloacal vertebrae: steeply inclined medially, 30° or more from the horizontal (0); moderately inclined medially, between 15-30° from the horizontal (1); not inclined medially, <15° from horizontal (2).

Supplemental References

Auffenberg, W. (1963). The fossil snakes of Florida. University of Florida, Florida State Museum.

Caldwell, M. W., & Albino, A. (2003). Exceptionally preserved skeletons of the Cretaceous snake *Dinilysia patagonica* Woodward, 1901. J. Vertebr. Paleontol. *22*, 861-866.

Caldwell, M. W., Nydam, R. L., Palci, A., & Apesteguía, S. (2015). The oldest known snakes from the Middle Jurassic-Lower Cretaceous provide insights on snake evolution. Nat. Commun. 6, 1-11.

Caldwell, M. W., Reisz, R. R., Nydam, R. L., Palci, A. & Simões, T. R. (2016) *Tetrapodophis amplectus* (Crato Formation, Lower Cretaceous, Brazil) is not a snake. SVP Book of Abstracts. Society of Vertebrate Paleontology, Meeting program & Abstracts of the 76th Annual meeting, 108-108.

Caldwell, M.W. (2019). The origins of snakes: morphology and fossil record. Boca Raton: Taylor & Francis. 327 p. ISBN 9781482251340.

Feldman, A., Sabath, N., Pyron, R. A., Mayrose, I., & Meiri, S. (2016). Body sizes and diversification rates of lizards, snakes, amphisbaenians and the tuatara. Global Ecol. Biogeogr. *25*, 187-197.

Garberoglio, F.F., Apesteguía, S., Simões, T.R., Palci, A., Gómez, R.O., Nydam, R.L., Larsson, H.C., Lee, M.S.Y. & Caldwell, M.W. (2019a). New skulls and skeletons of the

718 Cretaceous legged snake *Najash*, and the evolution of the modern snake body plan. Sci. Adv.
719 *5*, eaax5833.
720
721 Garberoglio, F. F., Gómez, R. O., Apesteguía, S., Caldwell, M. W., Sánchez, M. L., & Veiga,
722 G. (2019b). A new specimen with skull and vertebrae of *Najash rionegrina* (Lepidosauria:
723 Ophidia) from the early Late Cretaceous of Patagonia. J. Syst. Palaeontol. *17*, 1533-1550.
724
725
726 Gómez, R.O., Garberoglio, F.F. & Rougier, G.W. (2019). A new Late Cretaceous snake from
727 Patagonia: Phylogeny and trends in body size evolution of madtsoiid snakes. CR. Palevol.
728 *1136*, 1-11.
729
730 Hoffstetter, R., & Gasc, J. P. (1969). Vertebrae and ribs of modern reptiles. Biology of the
731 Reptilia, 1(5), 201-310.
732
733 Lanfear, R., Frandsen, P. B., Wright, A. M., Senfeld, T., & Calcott, B. (2017). PartitionFinder
734 2: new methods for selecting partitioned models of evolution for molecular and
735 morphological phylogenetic analyses. Mol. Phylogenetics Evol. *34*, 772-773.
736
737 Lewis, P. O. (2001). A likelihood approach to estimating phylogeny from discrete
738 morphological character data. Syst. Biol. *50*, 913-925.
739
740 Longrich, N. R., Bhullar, B. A. S., & Gauthier, J. A. (2012). A transitional snake from the
741 Late Cretaceous period of North America. *Nature*, *488*(7410), 205-208.
742

743 Maddison, W. P. (1991). Squared-change parsimony reconstructions of ancestral states for
744 continuous-valued characters on a phylogenetic tree. Syst. Biol. *40*, 304-314.
745
746 Maddison, W. P. and D.R. Maddison. (2019). Mesquite: a modular system for evolutionary
747 analysis. Version 3.61 http://www.mesquiteproject.org.
748
749 Onary, S., Fachini, T.S., Hsiou, A.S. (2017). The snake fossil record from Brazil. J. Herpetol.
750 *51*, 365-374.
751
752 Paparella, I., Palci, A., Nicosia, U., & Caldwell, M. W. (2018). A new fossil marine lizard
753 with soft tissues from the Late Cretaceous of southern Italy. R. Soc. Open Sci. *5*, 172411.
754
755 R Core Team. R: A language and environment for statistical computing. R Foundation for
756 Statistical Computing, Vienna, Austria. URL http://www.R-project.org/. (2013)
757 Rage, J.C. (1984). Part 11 Serpentes. In: Wellnhofer M, ed. Encyclopedia of
758 paleoherpetology. Germany: Gustav Fischer Verlag, 1–79
759 Rage, J.-C. & Escuillié, F. (2000). Un nouveau serpent bipède du Cénomanien (Crétacé).
760 Implications phylétiques. C. R. Acad. Sci. Paris (IIa) *330*, 513–520.
761 Ronquist, F., Teslenko, M., Van Der Mark, P., Ayres, D. L., Darling, A., Höhna, S., ... &
762 Huelsenbeck, J. P. (2012). MrBayes 3.2: efficient Bayesian phylogenetic inference and model
763 choice across a large model space. Syst. Biol. *61*, 539-542.
764 Siddall, M. E. (2010). Unringing a bell: metazoan phylogenomics and the partition bootstrap.
765 Cladistics *26*, 444-452.

766 Swofford, D. L. (2003). PAUP: phylogenetic analysis using parsimony, version 4.0 b10.

767 Tonini, J. F. R., Beard, K. H., Ferreira, R. B., Jetz, W., & Pyron, R. A. (2016). Fully-sampled
768 phylogenies of squamates reveal evolutionary patterns in threat status. Biol. Conserv. *204*,
769 23-31.

770 Zaher, H., Apesteguia, S., & Scanferla, C. A. (2009). The anatomy of the upper cretaceous
771 snake *Najash rionegrina* Apesteguía & Zaher, 2006, and the evolution of limblessness in
772 snakes. Zool. J. Linnean. Soc. *156*, 801-826.

773

774 Zheng, Y., & Wiens, J. J. (2016). Combining phylogenomic and supermatrix approaches, and
775 a time-calibrated phylogeny for squamate reptiles (lizards and snakes) based on 52 genes and
776 4162 species. Mol. Phylogenetics Evol. 94, 537-547.

777
778
779
780
781
782
783
784
785
786
787
788
789
790
791
792
793
794
795
796
797
798

Supplementary figures

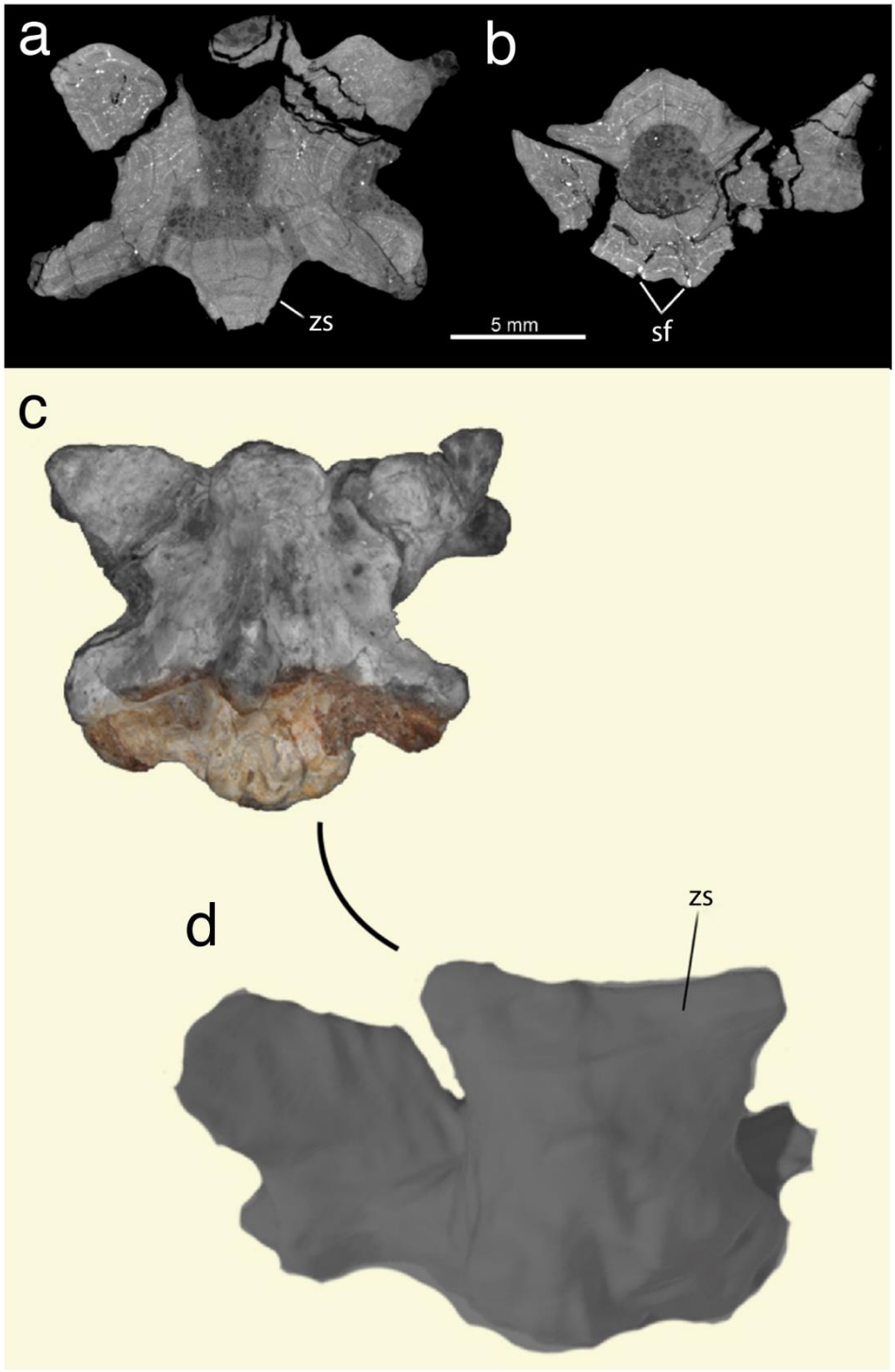

Fig. S1 Selected slices and reconstruction evidencing the morphology of *Boipeba tayasuensis*. Related to Fig. 1. a horizontal section through the anterior holotype vertebra showing the anterior edge of the zygosphene of the partial successive vertebra (anterior to the top). **b**. cross section through the holotype vertebra showing the presence of paired subcentral foramina. **c**. holotype evidencing the partial successive vertebra. **d**. three-dimensional

reconstruction of the partial successive vertebra showing the complete zygosphene roof morphology (anterior to the top). Sf., subentral foramina; ZS, zygosphene.

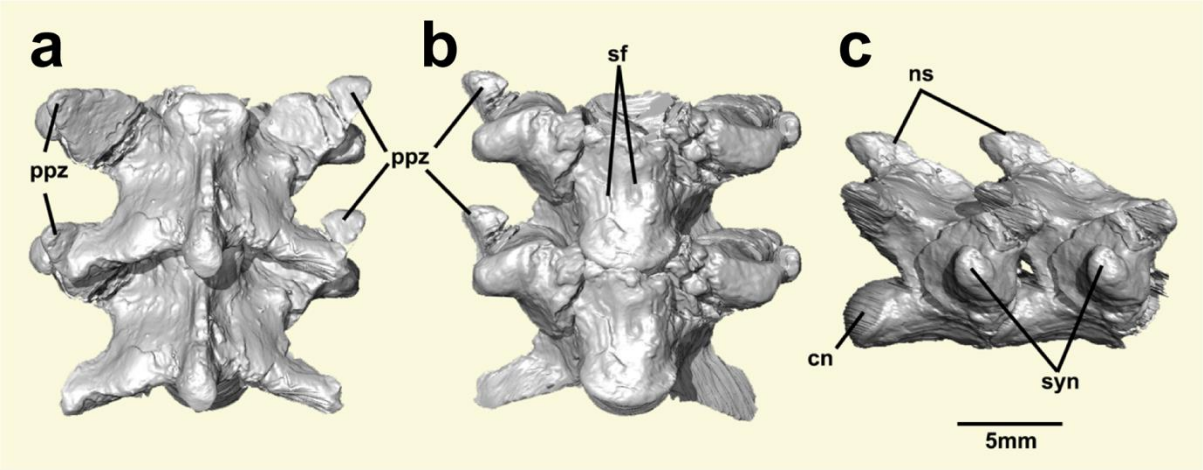

Fig. S2 Articulated sequence of digitally reconstructed vertebrae of *Boipeba tayasuensis*. Related to Fig. 2. a Dorsal view (anterior to the top). **b** Ventral view. **c** Right lateral view. This three-dimensional reconstruction is based on a digital replica articulated with the holotype. This image was generated with the free, open source software Blender v.2.79b. Note the distinct size of the elongated prezygapophyseal accessory processes of *Boipeba* protruding beyond the anterolateral margin of the prezygapophyseal facets. cn., condyle; ns., neural spine; ppz., prezygapophyseal accessory processes; sf., subcentral foramina; syn., synapophyses.

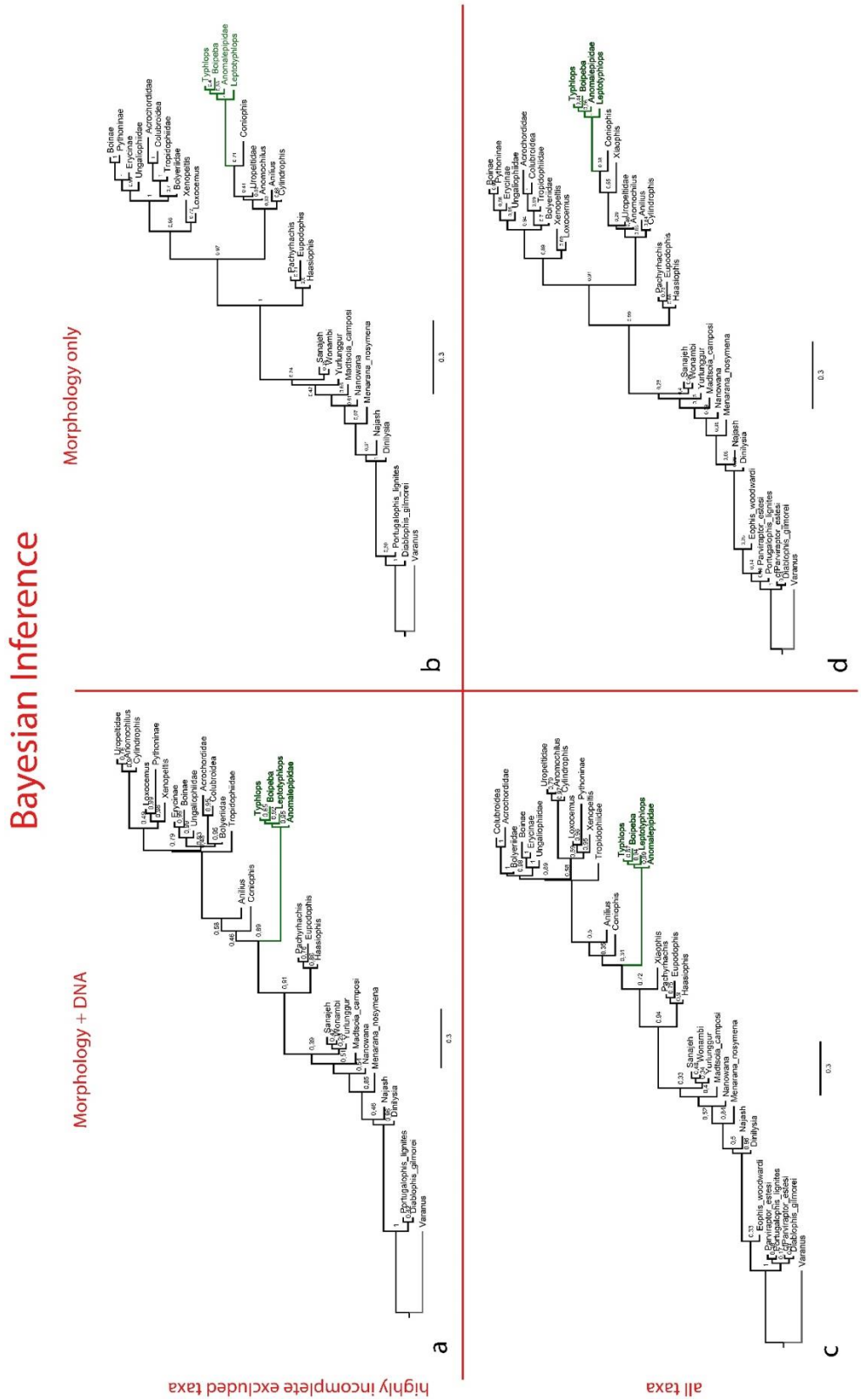

Fig. S3 Relationships of *Boipeba* and major snake lineages, based on Bayesian inference; majority-rule consensus trees from MrBayes. **Related to Fig. 4.** Numbers denote clade posterior probabilities. Scolecophidian (blindsnake) taxa in green. **a**. Morphology and DNA, with highly incomplete taxa excluded; **b**. Morphology only, with

853 highly incomplete taxa excluded; **c**. Morphology and DNA (all taxa); **d**. Morphology only
854 (all taxa).
855

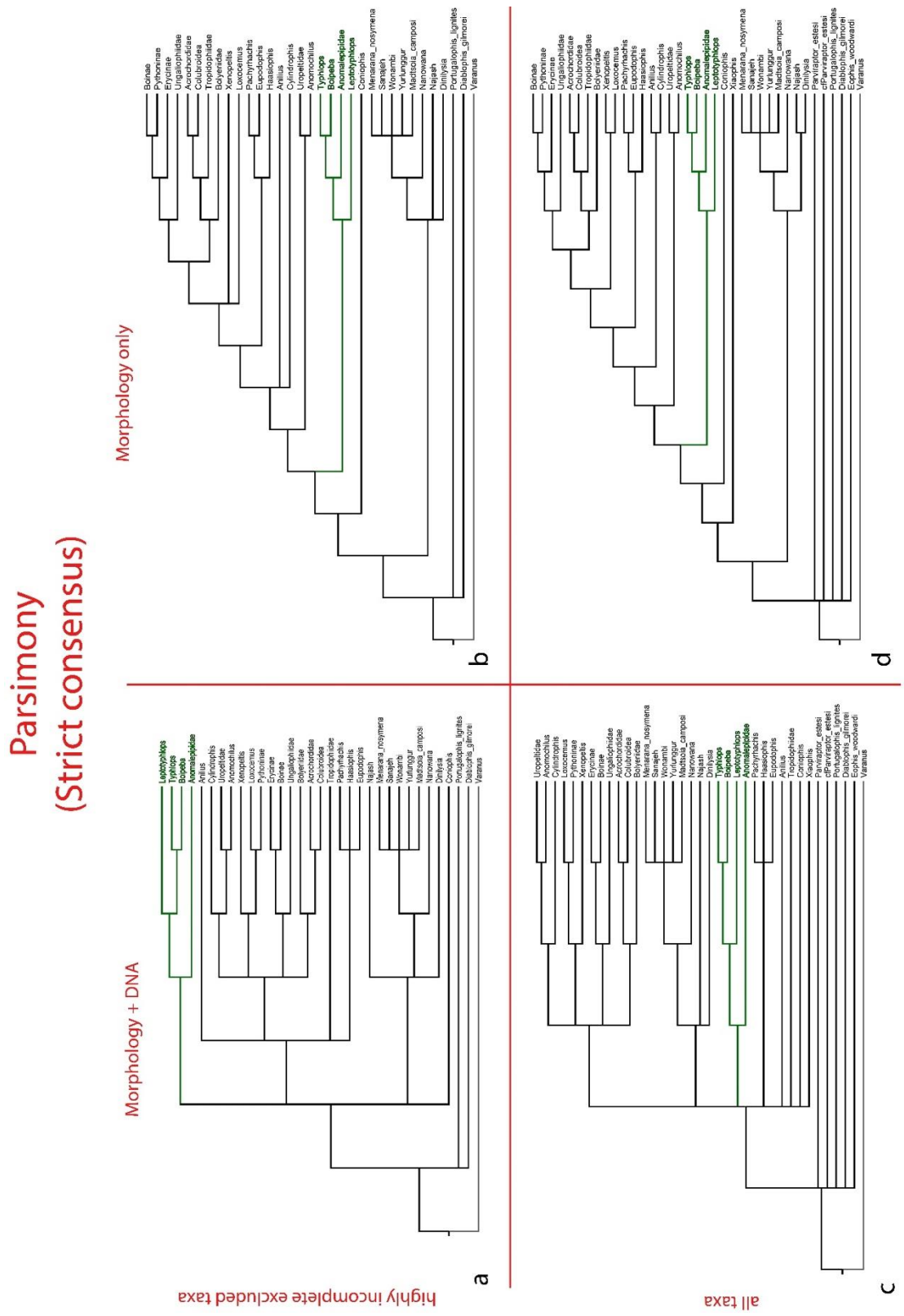

Fig. S4. Relationships of *Boipeba* and major snake lineages, based on parsimony analysis; strict consensus trees of shortest trees from PAUP. Related to Fig. 4. Scolecophidian (blindsnake) taxa in green. **a**. Morphology and DNA, with highly complete taxa excluded; **b**. Morphology only, with highly complete taxa excluded; **c**. Morphology and DNA (all taxa); and **d**. Morphology only (all taxa).

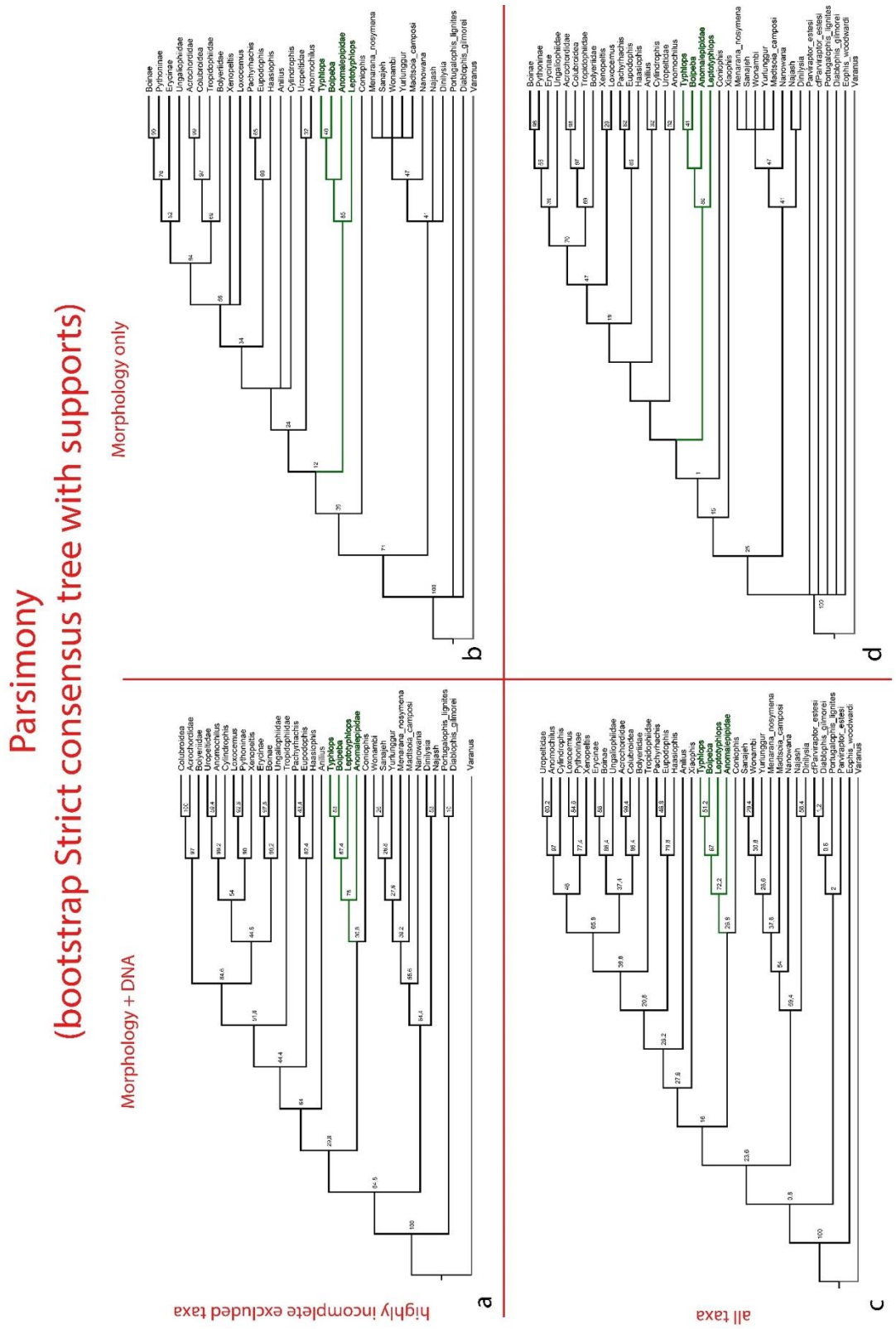

Fig. S5. Relationships of *Boipeba* and major snake lineages, based on parsimony analysis; majority-rule bootstrap consensus trees from TNT. Related to Fig. 4. Numbers denote bootstrap support for each clade. Scolecophidian (blindsnake) taxa in green. **a.** Morphology and DNA, with highly incomplete taxa excluded; **b.** Morphology only, with highly incomplete taxa excluded; **c.** Morphology and DNA (all taxa); **d.** Morphology only (all taxa).

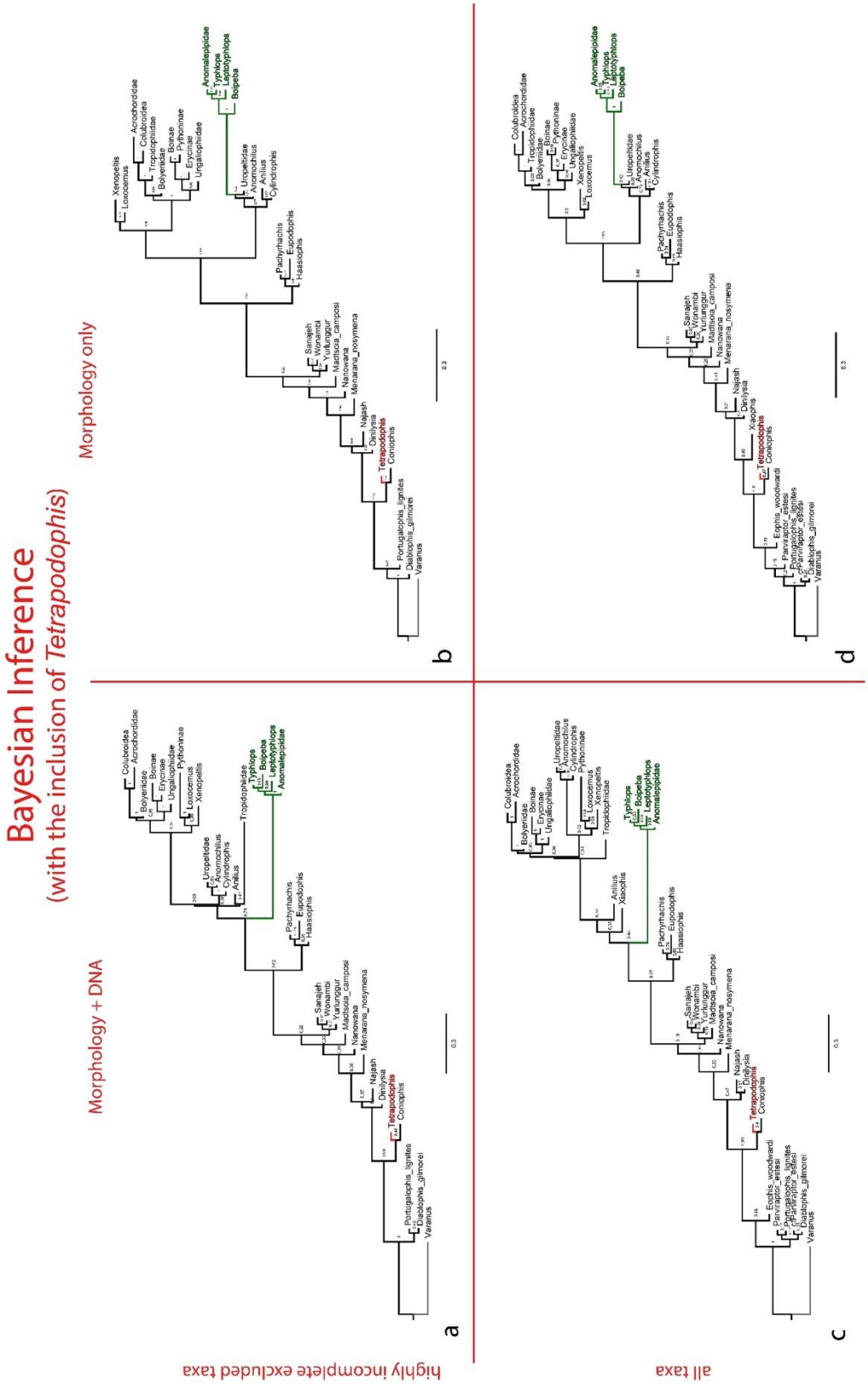

Fig. S6 Relationships of *Boipeba* and major snake lineages, based on Bayesian inference with the inclusion of the enigmatic and putative ophidian *Tetrapodophis amplectus*; majority-rule consensus trees from MrBayes. **Related to Fig. 4.** Numbers denote clade posterior probabilities. Scolecophidian (blindsnake) taxa in green. **a**. Morphology and DNA, with highly incomplete taxa excluded; **b**. Morphology only, with highly incomplete taxa excluded; **c**. Morphology and DNA (all taxa); **d**. Morphology only (all taxa)

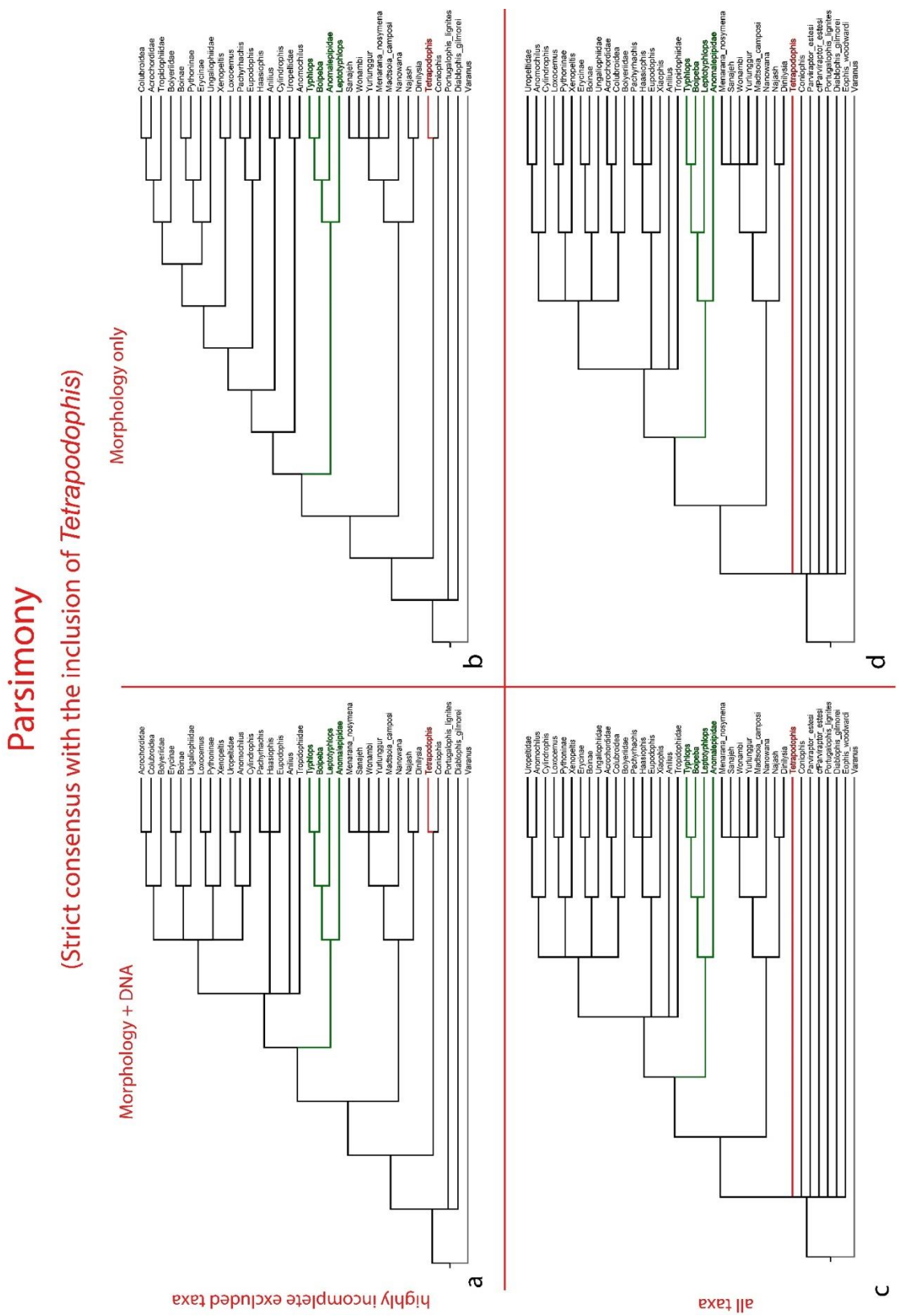

Fig. S7. Relationships of *Boipeba* and major snake lineages, based on parsimony analysis with the inclusion of the enigmatic and putative ophidian *Tetrapodophis amplectus*; strict consensus trees of shortest trees from PAUP. Related to Fig. 4. Scolecophidian (blindsnake) taxa in green. **a**. Morphology and DNA, with highly complete taxa excluded; **b**. Morphology only, with highly complete taxa excluded; **c**. Morphology and DNA (all taxa); and **d**. Morphology only (all taxa).

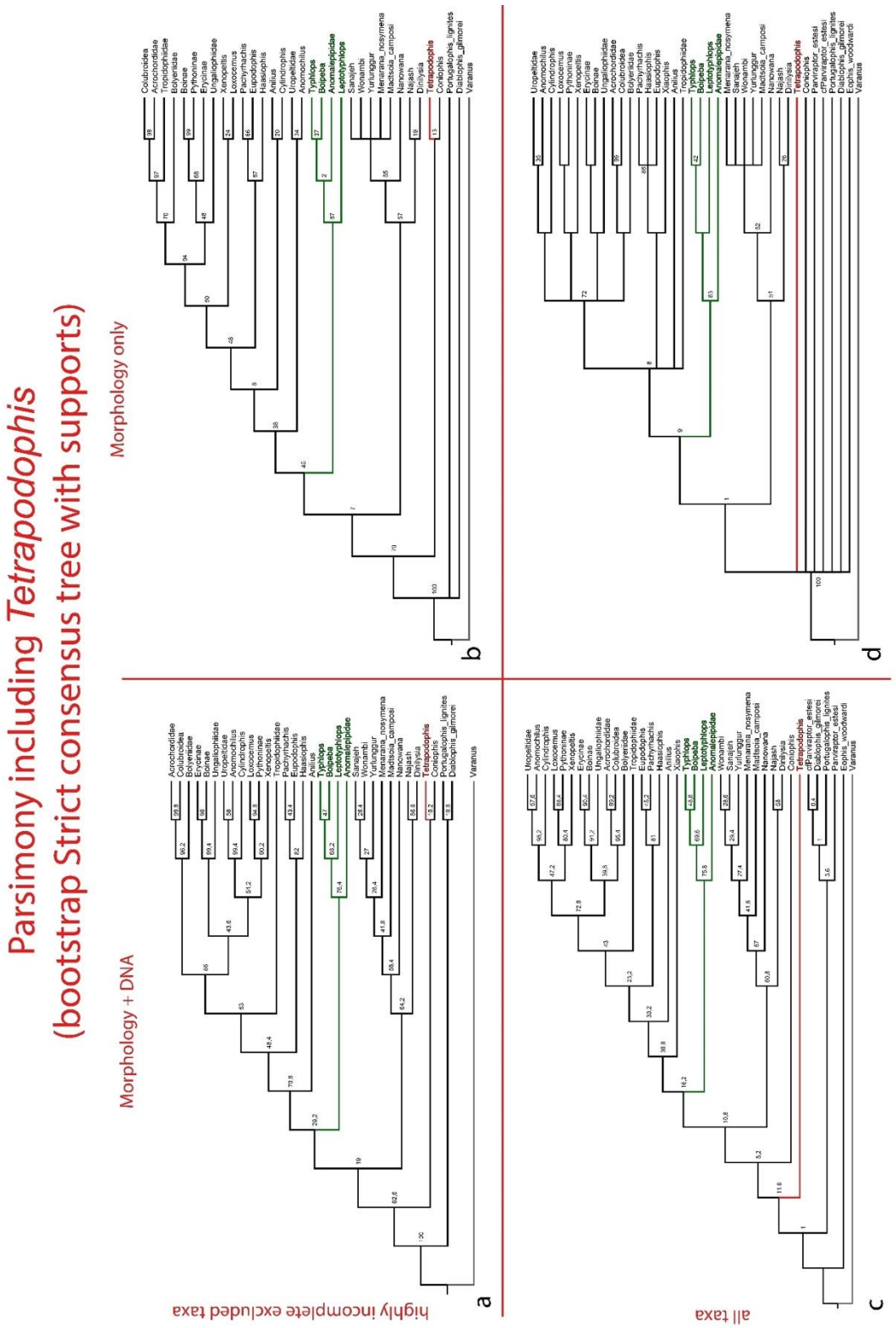

Fig. S8. Relationships of *Boipeba* and major snake lineages, based on parsimony analysis with the inclusion of the enigmatic putative ophidian *Tetrapodophis amplectus*; majority-rule bootstrap consensus trees from TNT. Related to Fig. 4. Numbers denote bootstrap support for each clade. Scolecophidian (blindsnake) taxa in green. **a.** Morphology and DNA, with highly incomplete taxa excluded; **b.** Morphology only, with highly incomplete taxa excluded; **c.** Morphology and DNA (all taxa); **d.** Morphology only (all taxa).

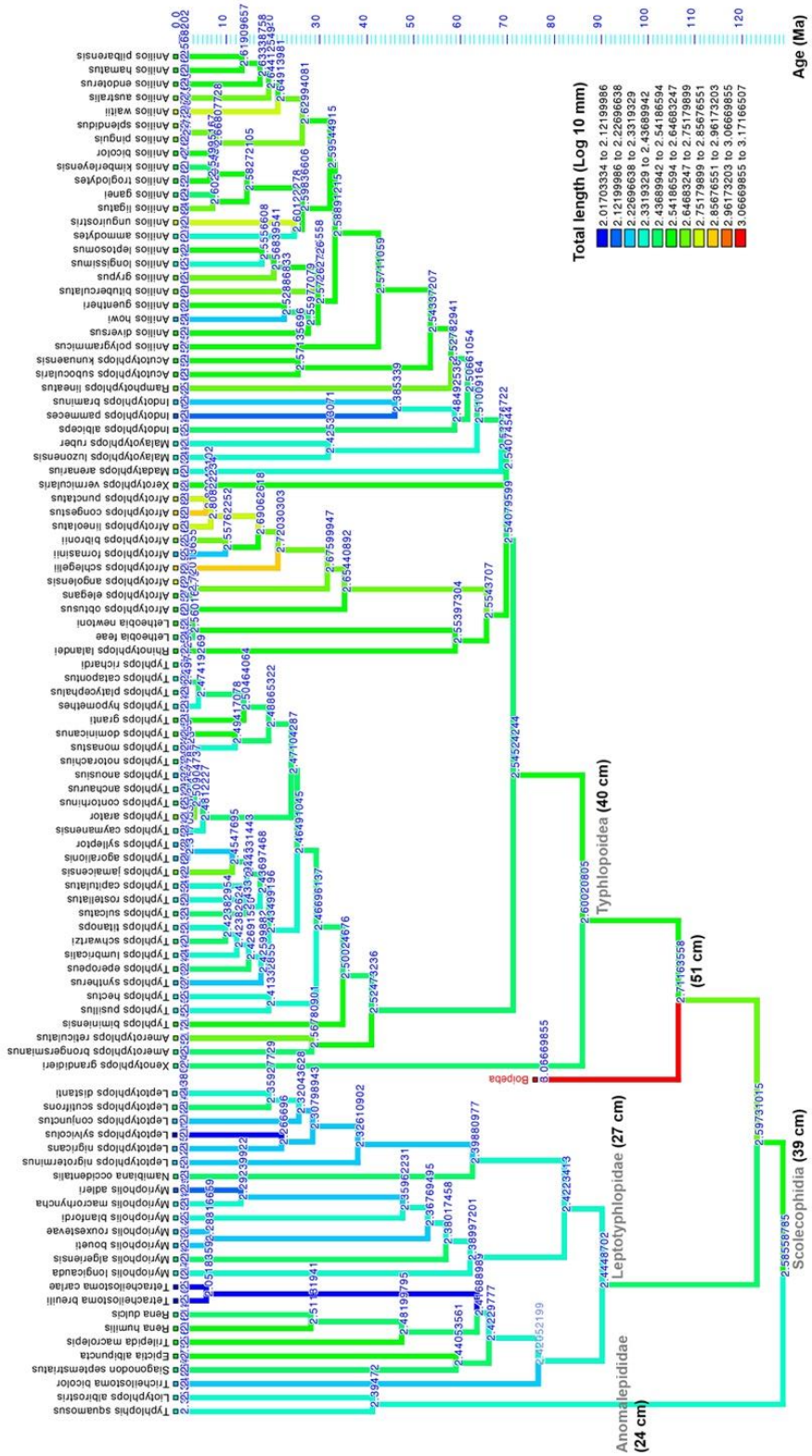

Fig. S9. Evolution of body size (total length) in scolecophidians. Related to Fig. 4. The analysis is based on squared-change parsimony with time-scaled branch lengths (=maximum likelihood with simple Brownian motion) in Mesquite. Warmer colours denote larger size. Numbers denote body length in mm (to $\log_{10}$ scale). For additional information consult Supplementary data 2.

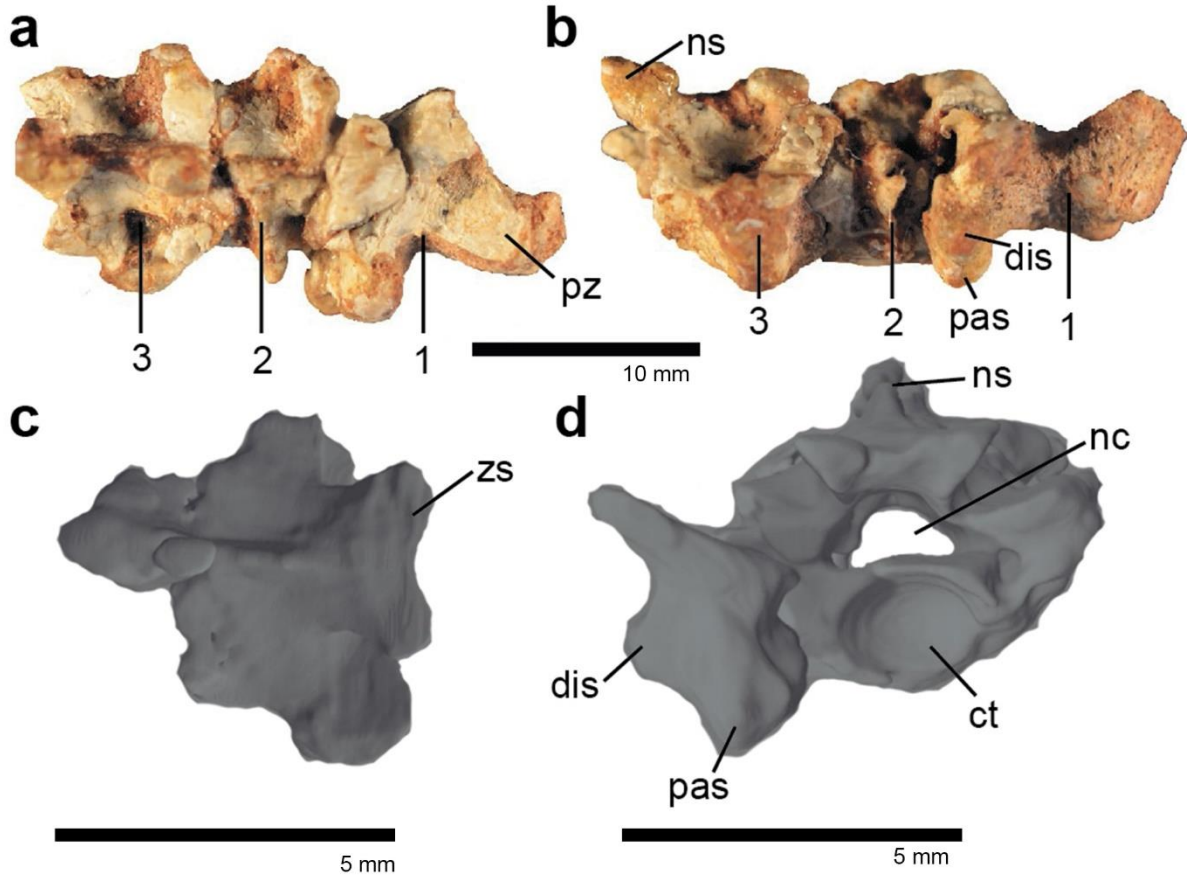

Figure S10. Set of three articulated vertebrae of indeterminate ophidian (unregistered specimen). **Related to Fig. 1. a** Dorsal view of the three articulated vertebrae (anterior to the right). **b** Lateral view (anterior to the right). **c** Dorsal view of digital reconstruction (i.e., segmented from micro CT) of posterior-most vertebra in the series (anterior to the right). **d** Anterior view of posterior-most vertebra in the series. Morphological differences from *Boipeba* include the concave anterior margin of the zygosphene, the distinctly trefoil-shaped cross section of the neural canal, and the presence of synapophyses subdivided into para- and diapophyseal facets. Abbreviations: dis, diapophyseal articular facet of the synapophysis; ct, cotyle; nc, neural canal; ns, neural spine; pas, parapophyseal articular facet of the synapophysis; pz, prezygapophysis; zs, zygosphene.